

AC3

GUGGENHEIM AERONAUTICAL LABORATORY

CALIFORNIA INSTITUTE OF TECHNOLOGY

AERODYNAMIC CHARACTERISTICS OF A WEDGE AND CONE
AT HYPERSONIC MACH NUMBERS

Thesis by

Lt. Lee R. Scherer, U.S.N.

1950

Thesis
S33

Thesis
S33

PASADENA, CALIFORNIA

Library
U. S. Naval Postgraduate School
Annapolis, Md.

AERODYNAMIC CHARACTERISTICS OF A WEDGE AND CONE
AT HYPERSONIC MACH NUMBERS

Thesis by
Lt. Lee R. Scherer, Jr., U.S.N

In Partial Fulfillment of the Requirements
For the Degree of
Aeronautical Engineer

California Institute of Technology
Pasadena, California

1950

12992

ACKNOWLEDGEMENTS

The author wishes to express his sincere appreciation to Dr. Henry T. Nagamatsu for his formulation of the problem and for his interest and guidance throughout the investigation.

Appreciation is also expressed to Mrs. Katherine McColgan, Aeronautics Librarian, whose patience and aid in ferreting out obscure references assisted materially in obtaining the necessary literature for this investigation, and to Miss Shirley Goodbury for her assistance in preparation of the manuscript.

The author is also indebted to his associate in the problem Lt. Richard D. DeJauer, USN.



ABSTRACT

Up to the present time, the reliability of the determination of aerodynamic characteristics at hypersonic Mach numbers by theoretical calculations has been unknown due to the lack of experimental data. This report is the calculations of these characteristics by four different theories of a wedge and a cone over a range of Mach numbers from 2 to 12.

Correlation of these results with wind tunnel tests was not possible due to scheduling difficulties of the hypersonic wind tunnel; therefore, this report is designed to serve as the basis for comparison of future hypersonic experiments.

From correlation of the various theories it is found that the closest agreement to the exact theory at hypersonic speeds is given by the hypersonic similarity theory. Above Mach numbers of about 3, the first and second order theories deviate considerably from the exact theory.



TABLE OF CONTENTS

<u>Part</u>	<u>Title</u>	<u>Page</u>
	Acknowledgments	1
	Abstract	ii
	Table of Contents	iii
	List of Figures	iv
	List of Tables	vi
	Symbols and Notation	viii
I.	Introduction	1
II.	Calculations by the Various Theories	3
	A. Oblique Shock Wave Theory for Wedge	3
	B. Exact Theory for Cone	4
	C. First Order Theory - Wedge	5
	D. First Order Theory - Cone	8
	E. Second Order Theory - Wedge	10
	F. Second Order Theory - Cone	10
	G. Hypersonic Similarity	13
III.	Conclusions	16
	References	18
	Tables	19
	Figures	41



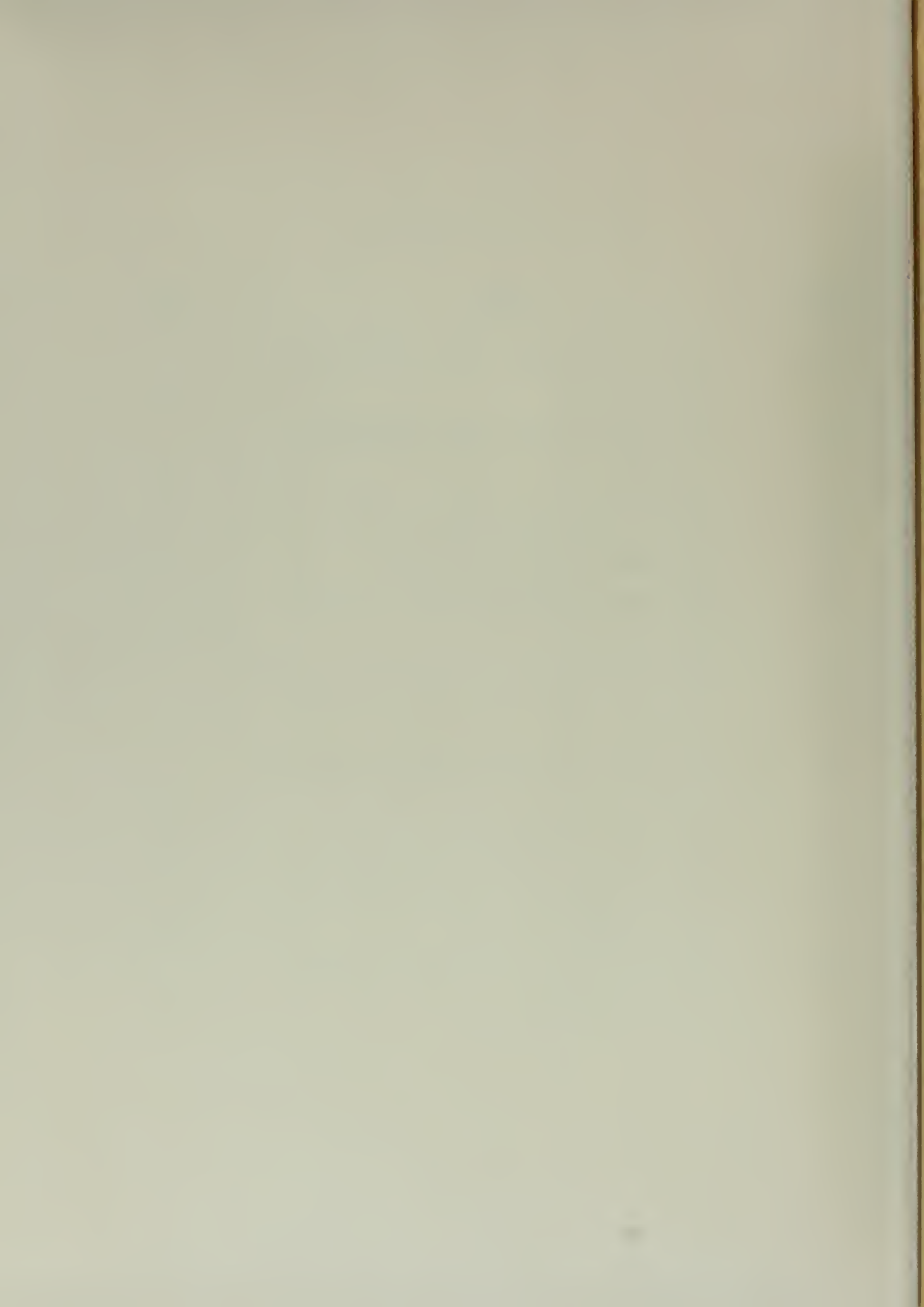
LIST OF FIGURES

<u>Figure No.</u>	<u>Title</u>	<u>Page</u>
1	Sketch of Wedge Model	41
2	Sketch of Cone Model	42
3	Photograph of Wedge Model	43
4	Photograph of Cone Model	43
5	Oblique Shock Theory - Wedge - 0° Angle of Attack, C_p vs M	44
6	Oblique Shock Theory - Wedge - 2° Angle of Attack, C_p vs M	45
7	Oblique Shock Theory - Wedge - 4° Angle of Attack, C_p vs M	46
8	Exact Theory - Cone, C_p vs M	47
9	First Order Theory - Wedge - 0° Angle of Attack, C_p vs M	48
10	First Order Theory - Wedge - 2° Angle of Attack, C_p vs M	49
11	First Order Theory - Wedge - 4° Angle of Attack, C_p vs M	50
12	First Order Theory - Cone, C_p vs M	51
13	Second Order Theory - Wedge - 0° Angle of Attack, C_p vs M	52



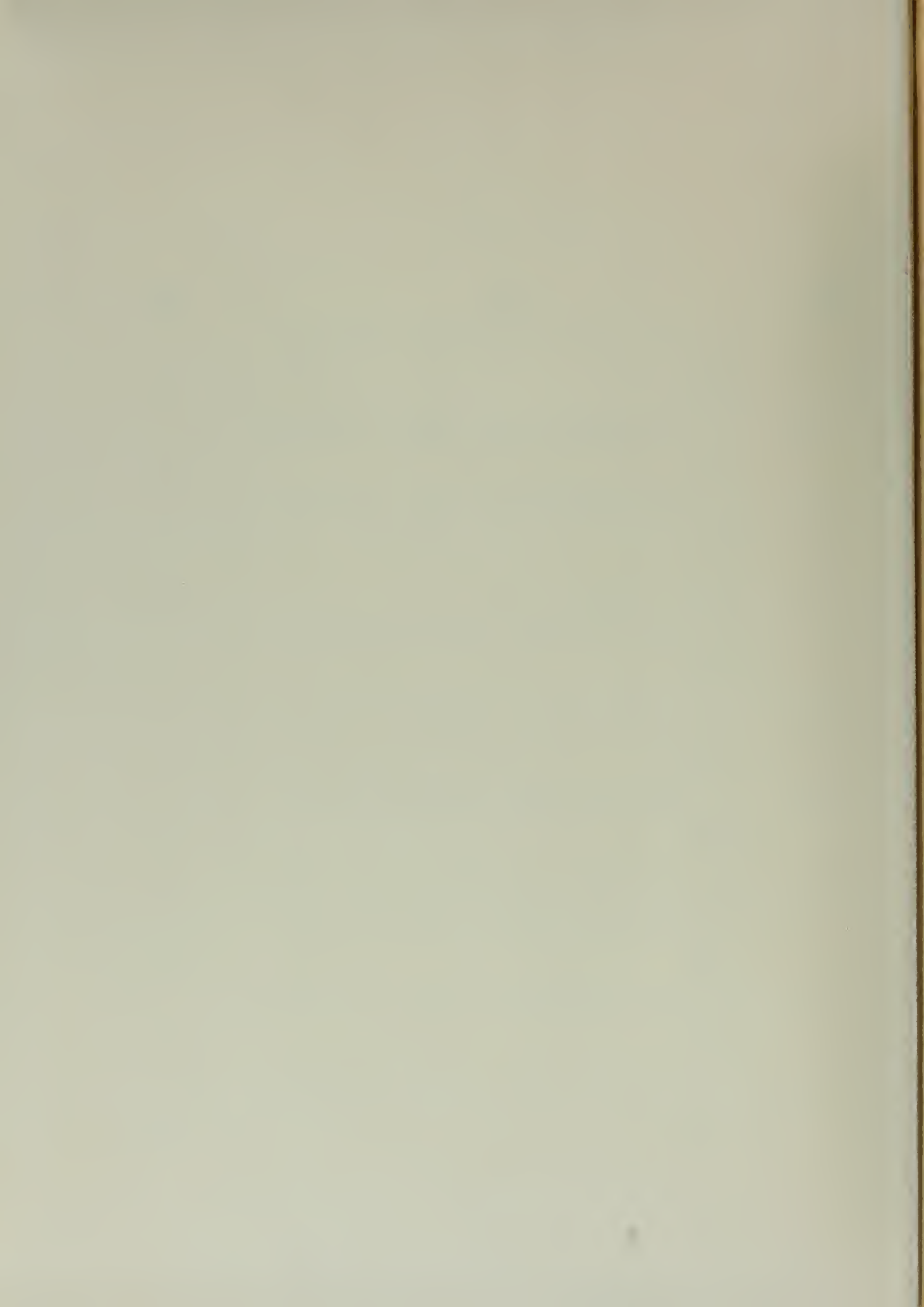
LIST OF FIGURES (continued)

<u>Figure No.</u>	<u>Title</u>	<u>Page</u>
14	Second Order Theory - Wedge - 2° Angle of Attack, C_p vs M	53
15	Second Order Theory - Wedge - 4° Angle of Attack, C_p vs M	54
16	Second Order Theory - Cone, C_p vs M	55
17	Hypersonic Similarity Parameters	56
18	Hypersonic Similarity - Wedge - 0° Angle of Attack, C_p vs M	57
19	Hypersonic Similarity - Wedge - 2° Angle of Attack, C_p vs M	58
20	Hypersonic Similarity - Wedge - 4° Angle of Attack, C_p vs M	59
21	Hypersonic Similarity - Cone, C_p vs M	60
22	Various Theories - 20° Wedge and Cone - 0° Angle of Attack, C_p vs M	61
23	Various Theories - 20° Wedge - 2° and 4° Angles of Attack, C_L vs M	62



LIST OF TABLES

<u>Table No.</u>	<u>Title</u>	<u>Page</u>
I	C_p , Oblique Shock Theory - Wedge - 0° Angle of Attack	19
II	C_p , Oblique Shock Theory - Wedge - 2° Angle of Attack	20
III	C_p , Oblique Shock Theory - Wedge - 4° Angle of Attack	21
IV	C_p , Exact Theory - Cone	22
V	C_p , First Order Theory - Wedge - 0° Angle of Attack	23
VI	C_p , First Order Theory - Wedge - 2° Angle of Attack	24
VII	C_p , First Order Theory - Wedge - 4° Angle of Attack	25
VIII	C_p , First Order Theory - Cone	26
IX	C_p , Second Order Theory - Wedge - 0° Angle of Attack	27
X	C_p , Second Order Theory - Wedge - 2° Angle of Attack	28
XI	C_p , Second Order Theory - Wedge - 4° Angle of Attack	29



LIST OF TABLES (continued)

<u>Table No.</u>	<u>Title</u>	<u>Page</u>
XII	C_p , Second Order Theory - Cone	30
XIII	Hypersonic Similarity Parameters	31
XIV	C_p , Hypersonic Similarity - Wedge - 0° Angle of Attack	32
XV	C_p , Hypersonic Similarity - Wedge - 2° Angle of Attack	33
XVI	C_p , Hypersonic Similarity - Wedge - 4° Angle of Attack	36
XVII	C_p , Hypersonic Similarity - Cone	39
XVIII	C_L , Various Theories - 20° Wedge	40



SYMBOLS AND NOTATION

The following are the symbols and notation with their definitions used in this investigation.

P_i	static pressure of the flow. The subscripts denote flow field
	1 - free stream
	2 - flow behind shock or on body
	o - stagnation conditions
	s - flow on surface of body
C_p	pressure coefficient = $\Delta P/q$
q	free stream dynamic pressure = $\frac{1}{2} \rho U^2 = \frac{\gamma P}{2} M^2$
u_1	free stream velocity
a_i	speed of sound $a_i = \sqrt{\frac{\delta p_i}{\rho_i}}$. Subscript indicates same conditions as pressure p
ρ_i	fluid density. Subscripts same as for p
M_i	Mach number = $\frac{u_i}{a_i}$. Subscripts same as p
β	inclination of shock wave, or the quantity $\sqrt{M_1^2 - 1}$
γ	ratio of specific heats - 1.4 for air
$r,$	cylindrical or spherical coordinates
x_i	Cartesian coordinates. Subscripts denote orthogonal directions of axis
u, v	velocity components

SYMBOLS AND NOTATION (continued)

u_i, v_k	indicate $\frac{\partial u}{\partial i}, \frac{\partial v}{\partial k}$ where i, k are coordinates of system being used
θ	semi-apex angle of cone or wedge, and flow deflection in one particular case
Φ	potential notation
α	angle of attack
ξ, η, t	non-dimensional coordinates, or variables of integration
δ	body thickness, or total apex angle
b	body length
k	thickness ratio parameter (δ/bM)

I. INTRODUCTION

The purpose of this investigation was to calculate the aerodynamic characteristics of a wedge and a cone at hypersonic Mach numbers by utilizing the existing theories, and to correlate these results with actual test data.

The possibility of extending existing supersonic flow theories to hypersonic speeds has been investigated only theoretically up to this time, due to the lack of experimental data at hypersonic Mach numbers. Now the existence of a hypersonic wind tunnel makes such test data available, and this investigation is the first step in the correlation of such data with the various theories. Since there are so many ramifications to the problem, boundary layer, tunnel boundary interference, deviations from a perfect gas, etc., this is but one small phase of the vast over-all problem, and it is hoped that it will serve as a basis for future experimental work.

The principal aerodynamic characteristic obtained was the surface pressure on various angles for wedges and cones at Mach numbers ranging from 2 to 12. The four existing theories used in the determination of the theoretical pressure distribution were:

1. Oblique Shock Theory for Wedge; Exact Theory for Cone
2. First Order Theory - Linearized
3. Second Order Theory



4. Hypersonic Similarity.

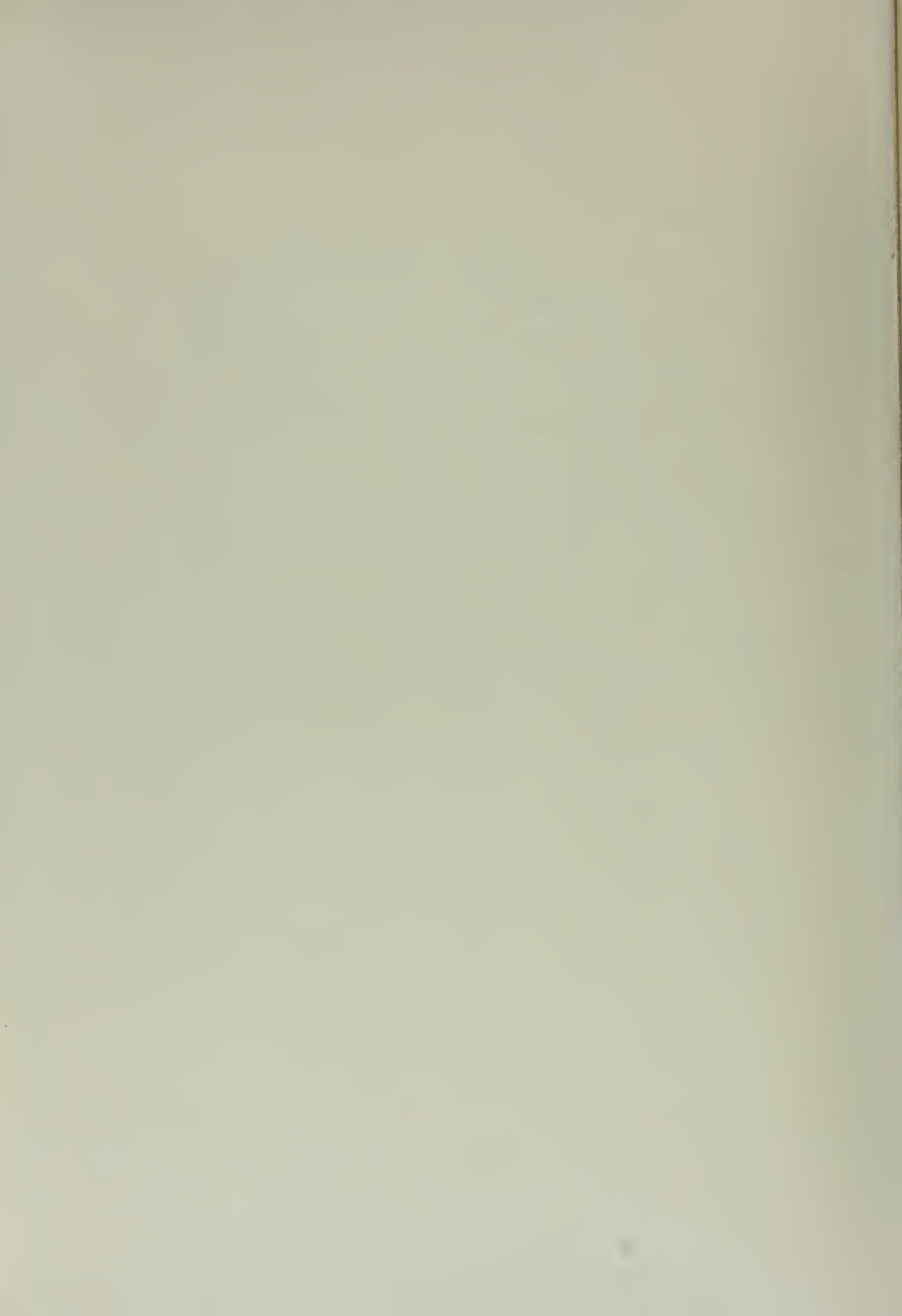
A brief discussion of the above theories is given in Part II.

For the theoretical calculations, the configurations used were:

1. Wedge with apex angles of 5° , 10° , 20° , 30° , 40° , 50° and 60° at angles of attack of 0° , 2° , and 4° .
2. Cone with apex angles of 5° , 10° , 20° , 30° , 40° , 50° and 60° at angle of attack of 0° .

Due to lack of time, actual correlation with test data was not possible in this report. Models of a 20° wedge and cone were constructed, and their details are included herewith.

It is planned that this report should serve as the first phase, the basic groundwork, for the future experimental investigations of hypersonic flow.



II. CALCULATIONS BY THE VARIOUS THEORIS

A. Oblique Shock Wave Theory for Wedge

The pressure coefficient (C_p) is defined as the ratio of the change in pressure (ΔP) to the dynamic pressure (q).

$$C_p = \frac{p_2 - p_1}{q}$$

but

$$q = \frac{1}{2} \rho U_1^2 = \frac{\gamma}{2} \rho_1 M_1^2$$

since

$$M_1 = \frac{U_1}{a_1} \quad \text{and} \quad a_1 = \sqrt{\frac{\gamma p_1}{\rho_1}}$$

Therefore,

$$C_p = \frac{\Delta p}{q} = \frac{2}{\gamma M_1^2} \frac{p_2 - p_1}{p_1}$$

The normal shock relation for $(p_2 - p_1)/p_1$ is $\frac{2}{\gamma + 1} (M_1^2 - 1)$.

To obtain the correct oblique shock relation, it is only necessary to replace M_1 by $M_1 \sin \beta$, (Ref. 1). Thus,

$$\frac{p_2 - p_1}{p_1} = \frac{2\gamma}{\gamma + 1} (M_1^2 \sin^2 \beta - 1)$$

$$C_p = \frac{4}{M_1^2 (\gamma + 1)} (M_1^2 \sin^2 \beta - 1)$$



Where the relation between the wave angle β and the flow deflection is

$$\frac{1}{M_1^2} = \sin^2 \beta - \frac{\gamma+1}{2} \frac{\sin \beta \sin \theta}{\cos(\beta-\theta)}$$

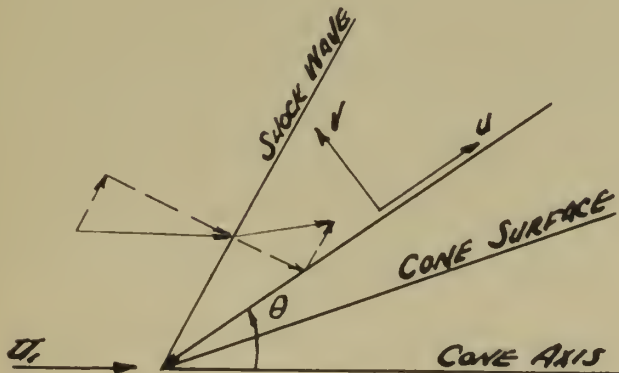
Utilizing this formula Tables I to III were computed and plotted in Figs. 5 to 7.

B. Exact Theory for Cone

The problem of supersonic flows around cones at zero angle of attack is one of the two types of high speed flows in three-dimensions that can be discussed mathematically without objectionable simplification.

The fundamental equation of conical flow as derived by Sebert in Ref. 2 and in a similar manner by Kopal, (Ref. 3), is

$$\frac{d^2 u}{d\theta^2} + u = \frac{a^2(u + v \cot \theta)}{V^2 - a^2}$$



The solutions to this equation cannot be obtained analytically, so in order to determine them, recourse must be had to numerical integration. This has been carried out by Kopal and put in tabular form. He tabulates the ratio of the pressure on the cone to that immediately behind the shock wave p_s/p_2 , and the ratio of the pressure immediately behind the shock wave, to that of the undisturbed air in front of the shock wave, p_2/p_1 . The product of these two gives p_s/p_1 so $\frac{\Delta P}{P_1}$ can be calculated, by

$$\frac{p_s}{p_1} - 1 = \frac{p_s - p_1}{p_1}$$

and

$$C_p = \frac{2}{\gamma M_1^2} \frac{p_s - p_1}{p_1}$$

Following this procedure the data of Table IV were calculated and plotted in Fig. 8.

C. First Order Theory - Wedge

By assuming irrotational flow and linearizing the equations of motion, a perturbation potential may be introduced. Considering a uniform rectilinear velocity U at ∞ , it is assumed that the deviations of the velocity from U are small, and squares and higher powers of these perturbation velocities are neglected. This assumption corresponds to limiting the solid boundaries to shapes whose inclination to U is always small.



The linearized equation of motion becomes, (Ref. 4)

$$\left(\frac{1-U^2}{Q_0^2}\right) \frac{\partial u_i'}{\partial x_i} + \frac{\partial u_2'}{\partial x_2} + \frac{\partial u_3'}{\partial x_3} = 0$$

where

(away from body)	(neighborhood of body)
$u_1 = U = \text{constant}$	$u_1 = U = u_1'$
$u_2 = 0$	$u_2 = u_2'$
$u_3 = 0$	$u_3 = u_3'$

In terms of the potential function

$$\phi = Ux_1 + \phi(x_i)$$

$$u_i = \frac{\partial \phi}{\partial x_i} \ll U$$

where $\phi(x_i)$ is the perturbation potential. The linearized perturbation potential equation becomes

$$(1-M_\infty^2) \frac{\partial^2 \phi}{\partial x_1^2} + \frac{\partial^2 \phi}{\partial x_2^2} + \frac{\partial^2 \phi}{\partial x_3^2} = 0$$

The same approximations are used for determining the pressure coefficient. The exact relationship for p/p_0 is

$$\frac{p}{p_0} = \left[\frac{1 - \frac{\gamma-1}{2} M_\infty^2}{1 + \frac{\gamma-1}{2} M^2} \right]^{\frac{\gamma}{\gamma-1}}$$

Linearized, this is

$$\frac{p_2}{p_1} = \frac{1}{1 + \frac{\gamma - 1}{2} M_1^2 \frac{2u'}{U}}$$

Expanding, we have

$$\frac{p_2}{p_1} = 1 - \frac{\gamma - 1}{2} M_1^2 \frac{2u'}{U} + \dots$$

Since

$$\frac{\gamma - 1}{2} M_1^2 p_1 = \frac{1}{2} \rho_1 U_1^2$$

thus,

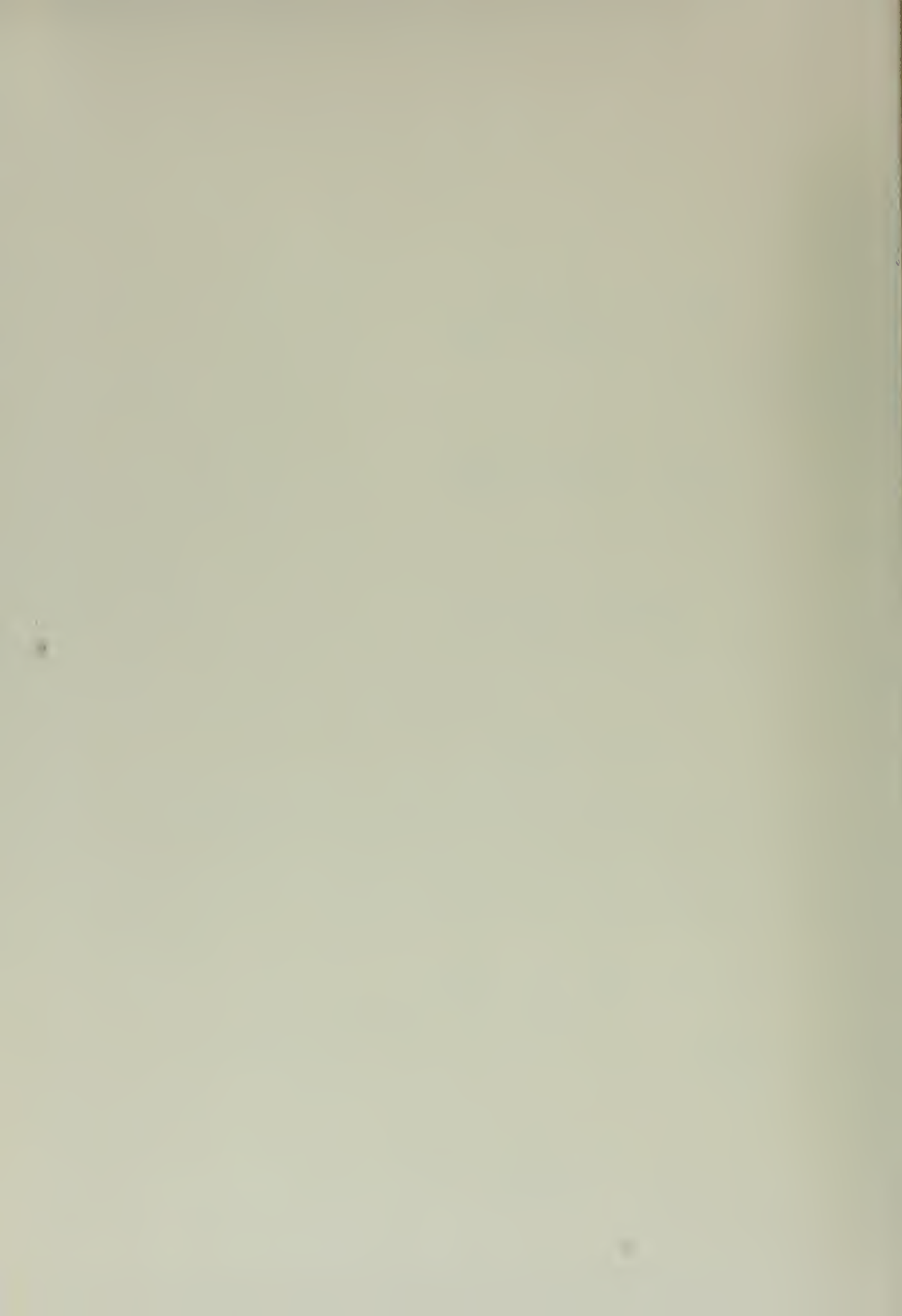
$$C_p = -2 \frac{u'}{U}$$

By solving the perturbation equation together with the boundary conditions that the normal derivative of ϕ vanishes at all solid boundaries, the pressure coefficient equation becomes

$$C_p = \frac{2}{\sqrt{M_1^2 - 1}} \left[\frac{dy_2}{dx_1} \right]_{\text{boundary}}$$

For the wedge $\left[\frac{dy_2}{dx_1} \right]_{\text{boundary}}$ is merely the tangent of the semi-apex angle θ , or

$$C_p = \frac{2}{\sqrt{M_1^2 - 1}} \tan \theta$$



For the wedge at angles of attack, this same equation holds by merely subtracting or adding α to Θ for the upper or lower surfaces.

These calculations are given in Tables V, VI, and VIII and are plotted in Figs. 9, 10, and 11.

D. First Order Theory - Cone

Following von Kármán, (Ref. 5), the linearized potential equation in cylindrical coordinates with axial symmetry is

$$\frac{d^2\phi}{dr^2} + \frac{1}{r^2} \frac{d\phi}{dr} + (1 - \frac{U^2}{a^2}) \frac{d^2\phi}{dx^2} = 0$$

Assuming that the effects of infinitesimals can be superimposed, the potential of the additional velocities has the form

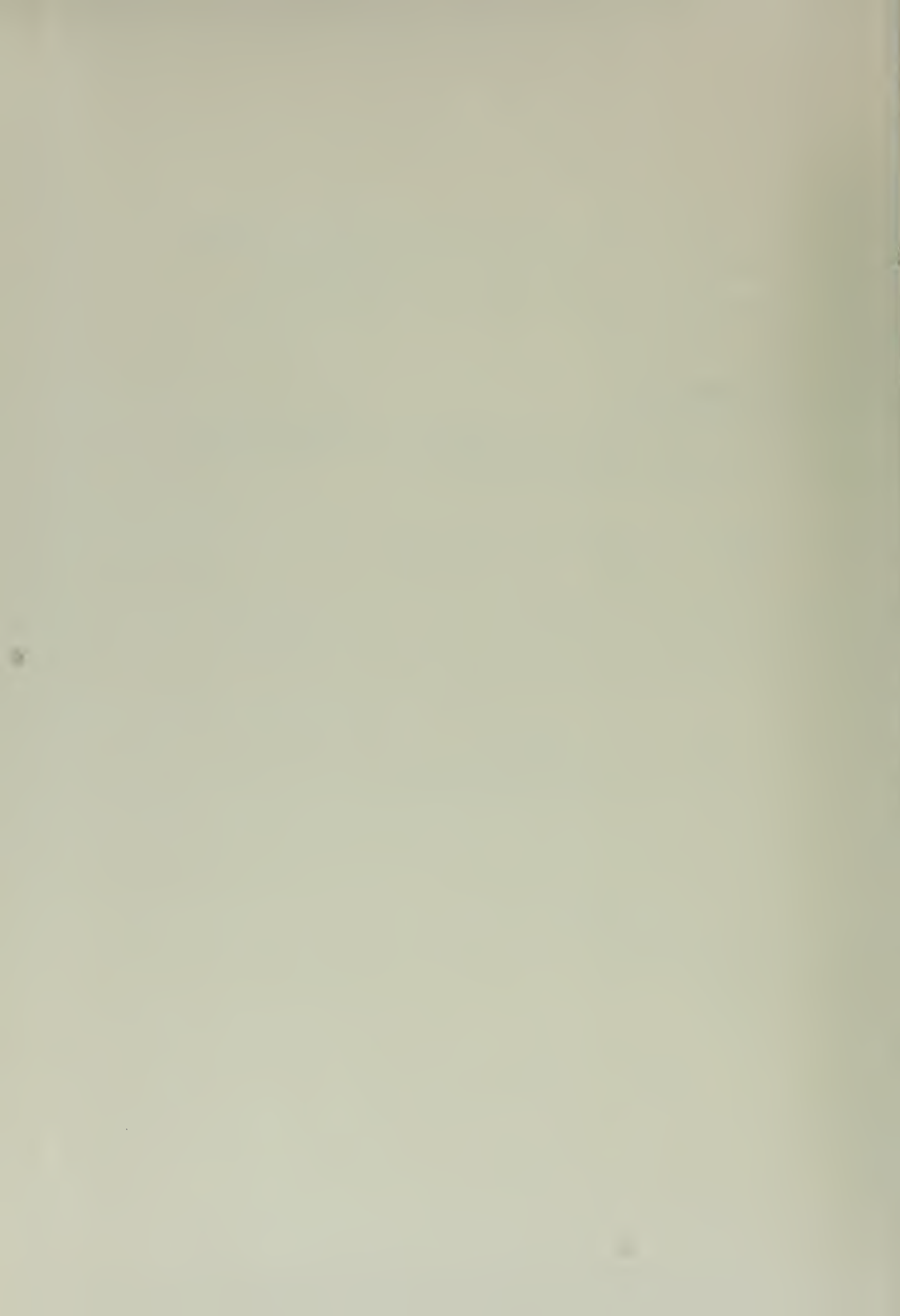
$$\phi(x, r) = \int_0^{x-\beta r} \frac{f(\xi) d\xi}{\sqrt{(x-\xi)^2 - \beta^2 r^2}}$$

where

$$\beta = \sqrt{M^2 - 1}$$

Placing the origin at the vertex of the body, this integral can be transformed by letting

$$\frac{x-\xi}{\beta r} = \cosh u$$



The potential expression becomes

$$\phi = \int_{\cosh \frac{x}{\beta r}}^0 f(x - \beta r) \cosh u \, du$$

and the velocity components are

$$\frac{\partial \phi}{\partial x} \quad \text{and} \quad \frac{\partial \phi}{\partial r}$$

By solving the above equation von Kármán obtained for the over pressure acting on the cone

$$\Delta p = \rho U^2 \theta^2 \frac{\cosh^{-1}(\frac{1}{\theta \beta})}{\sqrt{1 - \frac{\theta^2}{\beta^2} + \theta \cosh^{-1} \frac{1}{\theta \beta}}}$$

which is approximately

$$\Delta p = \rho U^2 \theta^2 \ln \left| \frac{2}{\theta \beta} \right|$$

Thus

$$C_p = 2 \theta^2 \ln \frac{2}{\theta \sqrt{M^2 - 1}}$$

The calculated results of this equation is given in Table VIII and plotted in Fig. 12.



E. Second Order Theory - Wedge

The next step to the linearization procedure used in the previous section in an iteration procedure corresponding to the general technique of solution by successive approximations based on the theory of perturbations, is the second approximation which may be made by several different approaches. By introducing a parameter τ proportional to the thickness ratio of the body under consideration, the potential function may be expanded in a power series in τ . This has been carried out by Busemann, (Ref. 6), for a two-dimensional supersonic flow.

The Busemann second approximation for the pressure coefficient is

$$C_p = \frac{\tau}{\sqrt{M^2-1}} \theta + \frac{\delta M^2 + (M^2-2)^2 \theta^2}{2(M^2-1)^2}$$

is the angle of flow deflection, the semi-apex angle at zero angle of attack. The computations based on this equation are given in Tables IX, X, and XI and are plotted in Figs. 13, 14, and 15.

F. Second Order Theory - Cone

For axially-symmetric flow, the discovery of a particular solution of the iteration equation has reduced the problem of determining a second-order approximation to one of first-order.



Following Van Dyke, (Ref. 7), the iteration equation for a cone

is

$$(1-t^2) \bar{\Phi}_{tt} + \frac{\bar{\Phi}_t}{t} = M^2 \left[2(N-1)t^2 \bar{\Phi}_{tt} (\bar{\Phi} - t\bar{\Phi}_t) - 2t\bar{\Phi}_{tt} + \bar{\Phi}_t + \beta^2 \bar{\Phi}_{tt} \bar{\Phi}_t^2 \right]$$

where (x, t) are the conical non-orthogonal coordinates and

$$t = \frac{\beta r}{x} \quad \beta = \sqrt{M^2 - 1} \quad N = \frac{(\delta + 1)M^2}{2\beta^2}$$

$$\bar{\Phi}(x, t, \theta) = x \bar{\Phi}(t, \theta)$$

$$\bar{\Phi}_r = \beta \bar{\Phi}_t$$

$$\bar{\Phi}_x = \bar{\Phi} - t \bar{\Phi}_t$$

$$\bar{\Phi}_{rr} = \frac{\beta^2}{x} \bar{\Phi}_{tt}$$

$$\bar{\Phi}_{xx} = \frac{t^2}{x} \bar{\Phi}_{tt}$$

$$\bar{\Phi}_{xr} = -\frac{\beta t}{x} \bar{\Phi}_{tt}$$

$\bar{\Phi}$ is first order perturbation potential

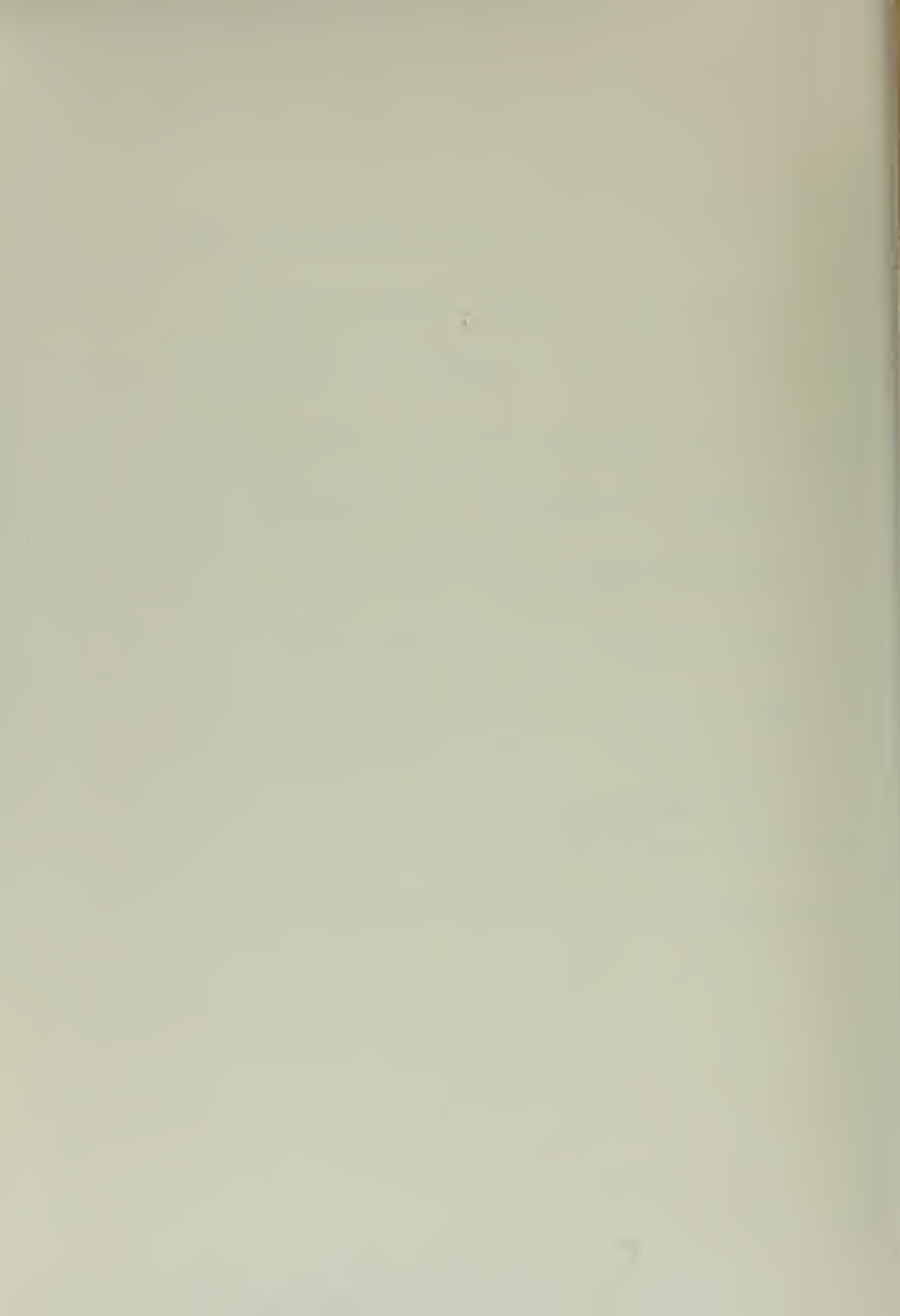
$\bar{\Phi}^{(2)} = \bar{\Phi} + \mathcal{O}$ is second order perturbation potential

The boundary conditions for the second order solution are

$$\frac{\bar{\Phi}_r}{1 + \bar{\Phi}_r} = \text{slope}$$

$$\beta \bar{\Phi}_t(\beta \epsilon) = \epsilon [\bar{\Phi}(\beta \epsilon) - \beta \epsilon \bar{\Phi}_t(\beta \epsilon)]$$

$$\bar{\Phi}(\infty) = \bar{\Phi}_t(\infty) = 0$$



The cone has a semi-apex angle $\tan^{-1} \epsilon$. Using the integrating factor

$\frac{t}{\sqrt{1-t^2}}$, the equation can be integrated to give the result

$$\bar{\Phi} = -A (\text{SECH}^{-1} t - \sqrt{1-t^2})$$

where $A = \frac{\epsilon^2}{\sqrt{1-\beta^2\epsilon^2} + \epsilon^2 \text{SECH}^{-1}(\beta\epsilon)}$

Substituting the first order solution into the iteration equation and using the same integrating factor again, Van Dyke obtains for the complete conical second-order perturbation potential

$$\begin{aligned} \bar{\Phi}^{(2)}(t) = & -A (\text{SECH}^{-1} t - \sqrt{1-t^2}) + AM^2 B (\text{SECH}^{-1} t - \sqrt{1-t^2}) \\ & + (\text{SECH}^{-1} t)^2 - (N+1) \sqrt{1-t^2} \text{SECH}^{-1} t - \frac{\beta^2 A \sqrt{1-t^2}}{4 t^2} \end{aligned}$$

The streamwise and radial velocity perturbations are

$$\begin{aligned} \frac{u}{U} = & -A \text{SECH}^{-1} t + A^2 M^2 B \text{SECH}^{-1} t + (\text{SECH}^{-1} t)^2 - (N-1) \frac{\text{SECH}^{-1} t}{\sqrt{1-t^2}} \\ & - (N+1) - \frac{3}{4} \beta^2 A \frac{\sqrt{1-t^2}}{t^2} \end{aligned}$$

$$\begin{aligned} \frac{1}{\beta} \frac{v}{U} = & A \frac{\sqrt{1-t^2}}{t} + A^2 M^2 \frac{-B \sqrt{1-t^2}}{t} - \frac{2 \sqrt{1-t^2} \text{SECH}^{-1} t}{t} + \frac{(N+1)}{t} \\ & + (N-1) t \frac{\text{SECH}^{-1} t}{\sqrt{1-t^2}} + \frac{1}{2} \beta^2 A \frac{\sqrt{1-t^2}}{t^3} \end{aligned}$$



B must be adjusted to satisfy the tangency condition. It is easiest to do this numerically in actual computation. From these results, the pressure coefficient can be calculated as

$$C_p = \frac{2}{\gamma M^2} \left\{ 1 - \frac{\gamma-1}{2} M^2 \left(1 - \frac{q^2}{U^2} \right)^{\frac{\gamma}{\gamma-1}} - 1 \right\}$$

These calculated values are given in Table XII and plotted in Fig. 16.

G. Hypersonic Similarity

Tsien, (Ref. 8), has developed the similarity laws for hypersonic flows. An affined transformation which expands the flow field laterally reduces the equations of the flows to a single non-dimensional equation. If a series of bodies having the same thickness distribution but different thickness ratio, δ/b , are put into flows of different Mach numbers M_1 such that the products of M_1 and δ/b remains constant and equal to K , then the flow patterns are similar in that they are governed by the same transformed velocity potential.

For flow over cones, Hayes, (Ref. 9), interpretation is the propagation of cylindrical waves from a uniformly expanding circular cylinder. To solve the associated wave problem, it is observed that the radial velocity v , the pressure p , and the density ρ are functions of $S = y/t$ only. That is,

$$\left(\frac{d}{dt} + \frac{y}{t} \frac{d}{dy} \right) (v, p, \rho) = 0$$

The equations of equilibrium and continuity become

$$(V-s) \frac{dV}{ds} = -\frac{1}{\rho} \frac{d\rho}{ds}$$

$$\frac{(V-s)}{\rho} \frac{d\rho}{ds} + \frac{dV}{ds} + \frac{V}{s} = 0$$

Introducing the following changes of variable

$$\mu = \frac{V}{s} \quad \beta = \frac{a^2}{s^2} \quad \sigma = \ln s$$

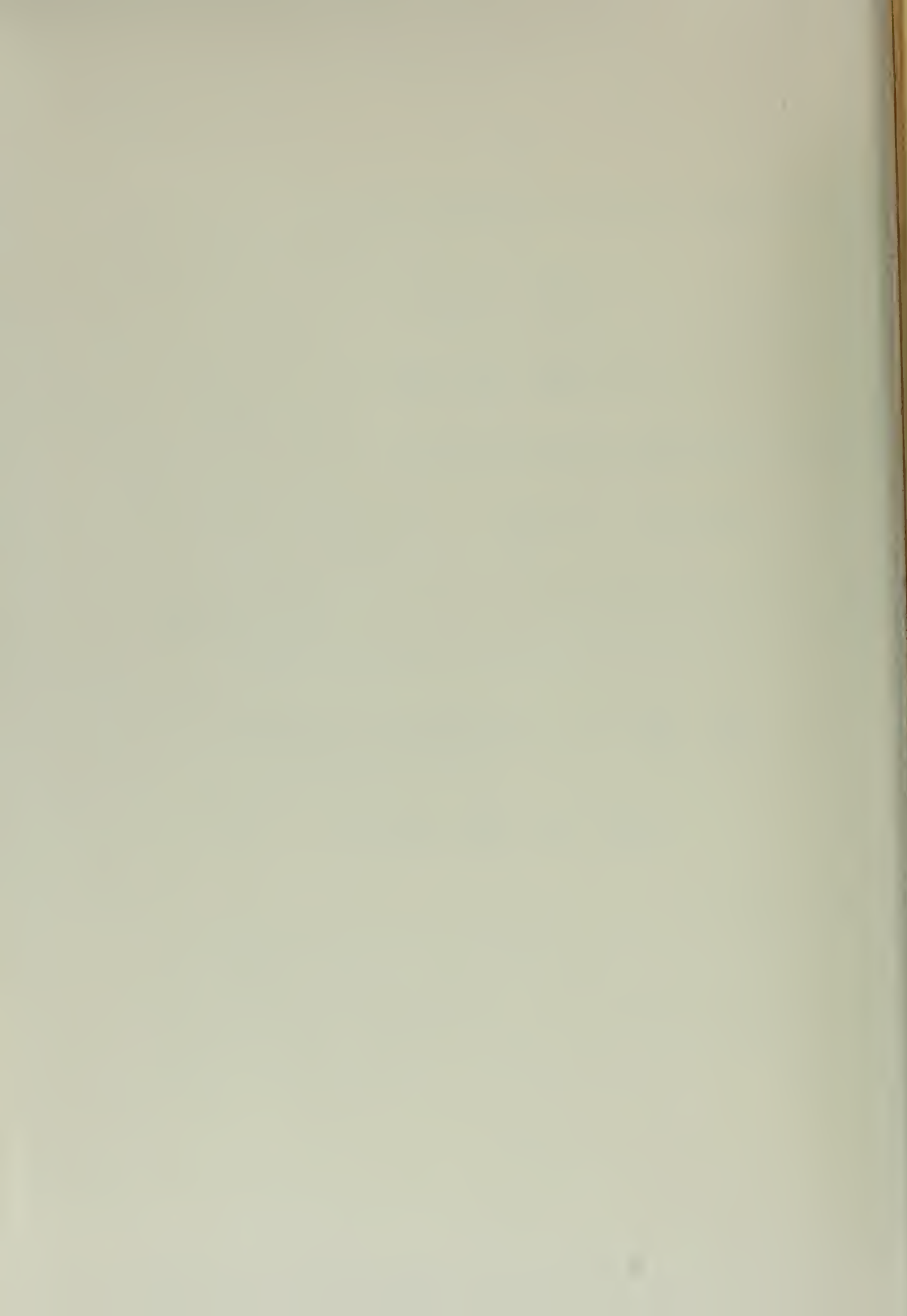
where μ is the new independent variable and "a" denotes the local velocity of sound, the equations above are transformed into

$$\frac{d\beta}{d\mu} = \frac{2\beta}{\mu} \beta + \frac{\frac{1}{2}(\gamma+1)\mu - 1(1-\mu)}{2\beta - (1-\mu)^2}$$

$$\frac{d\sigma}{d\mu} = -\frac{1}{\mu} \frac{\beta - (1-\mu)^2}{2\beta - (1-\mu)^2}$$

Shen, (Ref. 10), solves these basic equations by expanding the solution into a series near the initial point and using a standard numerical integration thereafter. From these results, the pressure ratio at the cone surface p_0/p_1 can be obtained. Calling the cone half-angle θ , we have

$$K = M_1 \theta$$



Now

$$C_p = \frac{2}{\gamma M_1^2} \left(\frac{P_5}{P_1} - 1 \right)$$

$$\frac{C_p}{\theta^2} = \frac{2}{\gamma K^2} \left(\frac{P_5}{P_1} - 1 \right)$$

Keeping the similarity parameter K constant will give the same flow pattern. Thus, a single curve of C_p/θ^2 vs K suffices for various slender cones in hypersonic flows.

Using Shen's tabulated results of K vs C_p/θ^2 it is a simple matter to expand to values of M and C_p for various θ_s . These results are given in Table XVI and are plotted in Fig. 21.

For hypersonic flow over wedges Shen's procedure gives

$$\frac{C_p}{\theta^2} = \frac{\gamma+1}{2} + 2 \sqrt{\left(\frac{\gamma+1}{4}\right)^2 + \frac{1}{K^2}}$$

Utilizing this equation, Table XIII of various values of C_p/θ^2 and K is obtained. These results are expanded as before for values of M and C_p for various θ_s . These data are given in Tables XIV, XV, and XVI and are plotted in Figs. 18, 19, and 20.

CONCLUSIONS

The conclusions of principal interest in the basic problem will result from the correlation of the experimental data with that calculated from the various existing theories. Since in this report such correlation is not as yet possible recourse must be had to a comparison of the various theories themselves.

For this purpose Fig. 22 has been plotted. This figure is a cross-plot of Mach number versus surface pressure coefficient as calculated by the various theories for the model wedge and cone, i.e., for a 20° total apex angle. From a study of this curve, the following conclusions may be drawn:

1. The first order theory gives values which are lower than those of the exact or oblique shock theory throughout the entire Mach number range. The amount of deviation increases with the Mach number.
2. The second order theory gives close agreement with the exact theory at low Mach numbers (below $M = 4$), and is much closer than the first order theory throughout the entire range.
3. The range over which first and second order theories may be used is limited by the form of the equations. This range is determined by the apex angle. For the 20° cone, imaginary results are obtained above Mach number of 11.0 by the first order theory and above Mach number of 5.7 by the second order theory.

4. At the higher Mach numbers (above 6) excellent agreement is obtained between the hypersonic similarity and exact solutions.

The lift coefficients for the 20° wedge at 2° and 4° angles of attack were calculated and plotted in Fig. 25. The same pattern of deviations between the exact and other theories is found as with the pressure coefficients.



REFERENCES

1. Millikan, C. E., "Hydrodynamics of Compressible Fluids", AE 261
Lecture Notes, California Institute of Technology, 1949-1950.
2. Sebert, Harold W., "High Speed Aerodynamics", Prentice-Hall, Inc.,
pp. 180-197, New York, 1948.
3. Kopal, Z., "Tables of Supersonic Flow Around Cones", Tech. Report
No. 1, Massachusetts Institute of Technology, Department of
Electrical Engineering, Center of Analysis, 1947.
4. Liepmann, H. W. and Puckett, A. E., "Aerodynamics of a Compressible
Fluid", GALCIT Aeronautical Series, John Wiley and Sons, Inc.,
pp. 121-124, New York, 1947.
5. Von Karman, Th., "The Problem of Resistance in Compressible Fluid",
Proc. of the 5th Volta Congress, pp. 275-277, Rome, 1936.
6. Busemann, A., "The Achsensymmetrische Kegel- und Kugelspitzenströmung",
Luftfahrtforschung, pp. 157-144, 1942.
7. Van Dyke, M. D., "A Study of Second-Order Supersonic Flow", Ph. D.
Thesis, California Institute of Technology, 1949.
8. Tsien, H. S., "Similarity Laws of Hypersonic Flows", Jour. of Math.
and Phys., Vol. 25, pp. 56-66, 1948.
9. Hayes, W. D., "On Hypersonic Similitude", Quart. of Appl. Math.,
Vol. 5, p. 105, 1947.
10. Shen, S. P., "Hypersonic Flow Over a Slender Cone", Jour. of Math.
and Phys., Vol. 27, pp. 56-66, 1948.



TABLE I

Wedge

Oblique Shock Theory

 0° Angle of Attack C_p δ

M	δ						
	5°	10°	20°	30°	40°	50°	60°
2.0	.0716	.110	.2565	.433	.665		
4.0	.0241	.0558	.1531	.2425	.379	.581	.738
6.0	.0177	.046	.106	.203	.329	.484	.666
8.0	.0148	.0525	.0939	.187	.3095	.463	.641
10.0	.0116	.0294	.0871	.1765	.302	.4515	.634
12.0		.028	.0835	.172	.295	.443	.625



TABLE II

Wedge

Oblique Shock Theory

2° Angle of Attack

M		δ						
		5°	10°	20°	30°	40°	50°	60°
2.0	C _p upper	.0133	.070	.192	.352	.556	.94	
	lower	.104	.168	.320	.51	.800		
4.0	C _p upper	.0045	.038	.100	.194	.324	.476	.652
	lower	.050	.086	.170	.293	.444	.612	.826
6.0	C _p upper	.0028	.026	.078	.162	.276	.420	.590
	lower	.040	.068	.142	.250	.384	.552	.742
8.0	C _p upper	.0022	.018	.068	.146	.260	.396	.566
	lower	.050	.082	.128	.236	.368	.530	.720
10.0	C _p upper	.0015	.012	.060	.140	.256	.390	.560
	lower	.026	.050	.120	.230	.360	.520	.710
12.0	C _p upper	.0011	.012	.060	.140	.256	.390	.560
	lower	.026	.050	.116	.250	.360	.520	.710

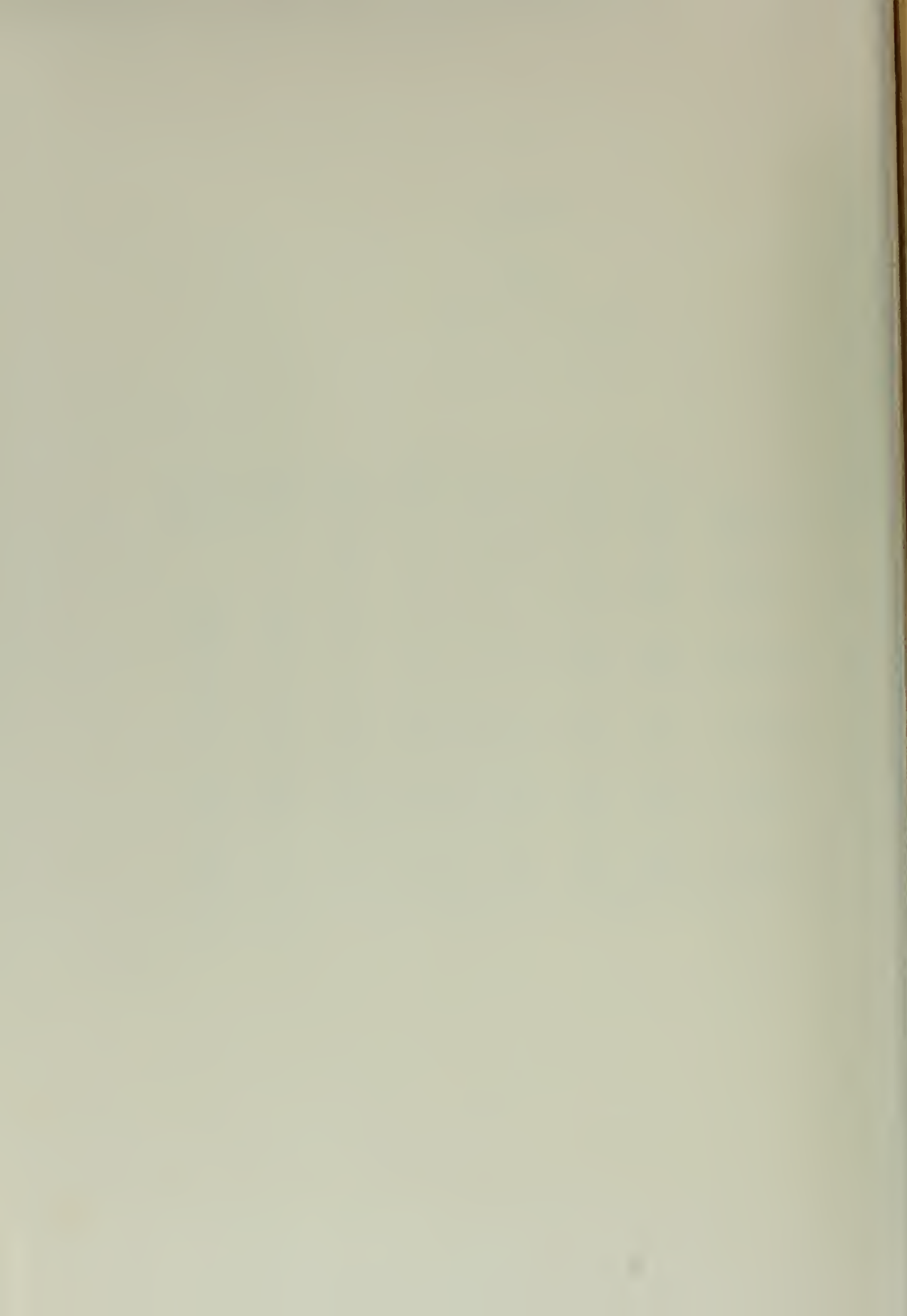


TABLE III

Wedge

Oblique Shock Theory

4° Angle of Attack

M		δ						
		5°	10°	20°	30°	40°	50°	60°
2.0	C_p upper		.025	.140	.290	.470	.720	
	lower	.154	.224	.390	.608			
4.0	C_p upper		.0109	.072	.150	.270	.414	.578
	lower	.080	.116	.220	.354	.506	.692	.924
6.0	C_p upper		.0069	.052	.124	.226	.380	.518
	lower	.060	.092	.184	.304	.450	.590	.830
8.0	C_p upper		.0042	.044	.110	.212	.340	.494
	lower	.050	.080	.170	.288	.428	.566	.800
10.0	C_p upper		.0040	.040	.104	.206	.354	.486
	lower	.044	.076	.160	.280	.420	.560	.790
12.0	C_p upper		.0037	.040	.100	.206	.330	.480
	lower	.044	.076	.160	.280	.420	.556	.786



TABLE IV

Cone

Exact Theory (Kopal)

 0° Angle of Attack C_p δ

M	δ					
	10°	20°	30°	40°	50°	60°
2.0	.0348	.1046	.2026	.3240	.473	.641
4.0	.0250	.0801	.1600	.2670	.382	.551
6.0	.0217	.0720	.1500	.2565	.375	.534
8.0	.0188	.0676	.1465	.2530	.365	.524
10.0	.0186	.0669	.1440	.2520	.363	.519
12.0	.0178	.0653	.1415	.2520	.363	.519



TABIE V

Wedge

First Order Theory

0° Angle of Attack

 C_p

M	δ						
	5°	10°	20°	30°	40°	50°	60°
2.0	.0505	.1006	.2025	.3090	.4200	.5230	.6650
4.0	.0225	.0449	.0909	.1530	.1680	.2410	.2975
6.0	.0148	.0295	.0596	.0900	.1232	.1500	.1955
8.0	.0110	.0219	.0443	.0672	.0914	.1172	.1450
10.0	.0082	.0175	.0355	.0532	.0732	.0939	.1160
12.0	.0073	.0140	.0293	.0443	.0608	.0780	.0965



TABLE VI

Wedge

First Order Theory

2° Angle of Attack

M		δ						
		5°	10°	20°	30°	40°	50°	60°
2.0	C_p upper	0	.0604	.1625	.2665	.3755	.4900	.6150
	lower	.0905	.1420	.2455	.3550	.4670	.5880	.7220
4.0	C_p upper	0	.0269	.0725	.1190	.1678	.2190	.2740
	lower	.0404	.0633	.1096	.1577	.2085	.2625	.3220
6.0	C_p upper	0	.0177	.0476	.0781	.1100	.1455	.1800
	lower	.0265	.0416	.0718	.1035	.1368	.1723	.2115
8.0	C_p upper	0	.0131	.0354	.0580	.0876	.1066	.1335
	lower	.0197	.0309	.0533	.0768	.1015	.1280	.1570
10.0	C_p upper	0	.0105	.0283	.0464	.0654	.0854	.1070
	lower	.0153	.0247	.0426	.0615	.0815	.1025	.1258
12.0	C_p upper	0	.0067	.0235	.0386	.0544	.0709	.0888
	lower	.0131	.0205	.0355	.0511	.0675	.0852	.1045



TABIZ VII

Wedge

First Order Theory

4° Angle of Attack

M		δ						
		5°	10°	20°	30°	40°	50°	60°
2.0	C _P upper	-.0302	.0201	.1214	.2240	.3315	.4430	.5630
	lower	.1312	.1830	.2880	.3975	.5140	.6390	.7780
4.0	C _P upper	-.0155	.0090	.0542	.1000	.1480	.1980	.2510
	lower	.0533	.0816	.1233	.1775	.2295	.2855	.3475
6.0	C _P upper	-.0089	.0059	.0356	.0656	.0970	.1300	.1650
	lower	.0385	.0356	.0844	.1165	.1503	.1875	.2230
8.0	C _P upper	-.0066	.0044	.0264	.0488	.0720	.0963	.1225
	lower	.0286	.0393	.0626	.0865	.1118	.1391	.1695
10.0	C _P upper	-.0053	.0035	.0212	.0391	.0577	.0772	.0980
	lower	.0229	.0319	.0502	.0693	.0893	.1115	.1358
12.0	C _P upper	-.0044	.0029	.0176	.0324	.0479	.0642	.0815
	lower	.0190	.0265	.0417	.0575	.0745	.0925	.1127

TABLE VIII

Cone

First Order Theory

 0° Angle of Attack C_p δ

M	δ						
	5°	10°	20°	30°	40°	50°	60°
2.0	.0134	.0394	.1148	.2036	.2932	.3720	.4400
4.0	.0094	.0268	.0658	.0950	.0952	.0646	
6.0	.0078	.0206	.0402	.0554			
8.0	.0066	.0162	.0220				
10.0	.0058	.0127	.0080				
12.0	.0031	.0099					

TABLE IX

Wedge

Second Order Theory

 0° Angle of Attack C_p δ

M	δ						
	5°	10°	20°	30°	40°	50°	60°
2.0	.0531	.1065	.2460	.4020	.5810	.7620	1.0000
4.0	.0253	.0519	.1276	.2190	.3500	.4590	.6070
6.0	.0170	.0371	.0960	.1721	.2651	.3775	.5087
8.0	.0133	.0300	.0808	.1481	.2346	.3488	.4625
10.0	.0111	.0257	.0720	.1559	.2168	.3201	.4352
12.0	.0096	.0229	.0660	.1257	.2045	.3108	.4165



TABLE X

Wedge

Second Order Theory

2° Angle of Attack

M		δ						
		5°	10°	20°	30°	40°	50°	60°
2.0	C _p upper	.0101	.0644	.1898	.3371	.5070	.6990	.9160
	lower	.0996	.1627	.5054	.4717	.6600	.8695	1.1040
4.0	C _p upper	.0045	.0304	.0960	.1803	.2832	.4050	.5460
	lower	.0480	.0811	.1615	.2614	.3795	.5161	.6720
6.0	C _p upper	.0030	.0233	.0709	.1389	.2255	.3306	.4554
	lower	.0340	.0593	.1236	.2069	.3085	.4232	.5655
8.0	C _p upper	.0022	.0165	.0586	.1189	.1978	.2954	.4118
	lower	.0271	.0486	.1053	.1809	.2744	.3862	.5162
10.0	C _p upper	.0018	.0133	.0515	.1075	.1820	.2743	.3863
	lower	.0232	.0424	.0946	.1657	.2547	.3622	.4873
12.0	C _p upper	.0015	.0121	.0468	.0994	.1707	.2603	.3693
	lower	.0204	.0383	.0874	.1554	.2411	.3457	.4675



TABLE XI

Wedge

Second Order Theory

4° Angle of Attack

M		δ						
		5°	10°	20°	30°	40°	50°	60°
2.0	C _p upper	-.0292	.0205	.1369	.2752	.4557	.6220	.8265
	lower	.1497	.2113	.3685	.5446	.7400	.9600	1.2010
4.0	C _p upper	-.0127	.0094	.0674	.1441	.2596	.3555	.4875
	lower	.0742	.1112	.1990	.3070	.4316	.5760	.7388
6.0	C _p upper	-.0081	.0063	.0487	.1094	.1884	.2872	.4035
	lower	.0539	.0830	.1544	.2450	.3541	.4815	.6266
8.0	C _p upper	-.0058	.0048	.0395	.0927	.1640	.2551	.3632
	lower	.0441	.0692	.1330	.2163	.3172	.4367	.5740
10.0	C _p upper	-.0045	.0039	.0342	.0850	.1499	.2358	.3395
	lower	.0385	.0613	.1206	.1995	.2952	.4098	.5422
12.0	C _p upper	-.0036	.0033	.0307	.0763	.1401	.2222	.3237
	lower	.0344	.0538	.1121	.1878	.2805	.3921	.5217

TABLE XI

Case

Second Order Theory

$\delta = 10^\circ$		$\delta = 20^\circ$		$\delta = 30^\circ$		$\delta = 40^\circ$	
M	C_p	M	C_p	M	C_p	M	C_p
3.04	.0253	2.14	.1010	1.60	.2270	1.70	.5476
7.68	.0207	3.01	.0381	2.68	.1837	2.80	.3155
11.36	.0209	3.91	.0824	3.83	.1829		
		5.48	.0821				
		5.70	.0829				

TABLE VIII

Hypersonic Similarity Parameters

Wedge		Cone (Ref. 8)	
K	C_p/e^2	K	C_p/e^2
.1	15.200	.60	2.95
.2	11.290	.92	2.65
.3	7.990	1.22	2.45
.4	6.560	1.59	2.31
.5	5.880	2.10	2.20
.6	4.740	2.74	2.14
.8	3.980	4.00	2.10
1.0	3.536		
1.5	2.992		
2.0	2.762		
3.0	2.762		
4.0	2.500		
5.0	2.464		
6.0	2.446		
7.0	2.452		

TABLE XIV

Wedge

Hyperbolic Similarity

0° Angle of Attack

5° δ		10° δ		20° δ		30° δ		40° δ		50° δ		60° δ	
M	C _p	M	C _p	M	C _p	M	C _p	M	C _p	M	C _p	M	C _p
2.80	.0289	2.29	.0369	1.70	.249	1.87	.388	2.20	.454	2.14	.778	1.75	1.17
4.59	.0234	3.43	.0615	2.27	.198	2.24	.841	2.75	.402	3.22	.655	2.62	1.00
6.86	.0152	4.57	.0490	2.83	.168	2.99	.287	4.12	.841	4.29	.605	3.49	.916
9.16	.0121	5.71	.0415	3.40	.148	3.74	.254	5.50	.515	6.44	.565	5.23	.857
11.45	.0102	6.86	.0565	4.54	.124	5.60	.215	8.25	.294	8.59	.548	6.99	.830
		9.15	.0306	5.67	.111	7.46	.199	11.00	.285	10.70	.540	8.72	.819
		11.40	.0272	8.50	.0984	11.40	.186					10.45	.812
												12.20	.808

TABLE XV

Wedge

Hypersonic Similarity

 2° Angle of Attack

$5^\circ \delta$				$10^\circ \delta$			
M	C_{Pu}	M	C_{PL}	M	C_{Pu}	M	C_{PL}
11.50	.00115	2.50	.0710	1.92	.041	1.63	.170
		3.80	.0530	3.85	.030	2.44	.120
		5.06	.0400	5.76	.022	3.25	.096
		6.32	.0336	7.70	.017	4.06	.081
		7.60	.0282	9.60	.014	4.89	.071
		10.20	.0250	11.50	.013	6.50	.060
		12.60	.0223			8.14	.054
						12.20	.045

TABLE XV (continued)

Wedge

Hypersonic Similarity

 2° Angle of Attack

$20^\circ \delta$				$30^\circ \delta$			
M	C_{P_u}	M	C_{P_L}	M	C_{P_u}	M	C_{P_L}
2.15	.160	1.83	.239	2.16	.235	1.96	.445
2.84	.127	2.55	.245	2.60	.251	2.62	.374
3.55	.103	2.82	.215	3.46	.211	3.28	.332
4.26	.095	3.76	.181	4.34	.187	4.90	.281
5.78	.080	4.70	.161	6.50	.159	6.54	.259
7.10	.071	7.04	.136	8.65	.146	9.80	.242
10.60	.060	9.40	.125	10.80	.137	13.20	.235
		14.00	.117				

TABLE XV (continued)

Wedge

Hypersonic Similarity

 2° Angle of Attack

$40^\circ \delta$				$50^\circ \delta$			
M	C_{Pu}	M	C_{PL}	M	C_{Pu}	M	C_{PL}
2.39	.422	1.98	.654	1.88	.720	1.96	.925
3.00	.575	2.47	.580	2.35	.640	2.94	.780
4.53	.317	3.71	.490	3.53	.540	3.92	.721
5.96	.293	4.95	.453	4.70	.500	5.89	.694
8.95	.274	7.42	.424	7.06	.466	7.85	.654
12.00	.265	9.90	.410	9.40	.453	9.80	.646
		12.30	.404	11.75	.445	11.75	.640

$60^\circ \delta$			
M	C_{Pu}	M	C_{PL}
1.88	1.010	2.40	1.170
2.82	.850	3.20	1.080
3.75	.786	4.80	1.010
5.73	.735	6.40	.980
7.50	.712	8.00	.964
9.40	.700	9.60	.960
11.20	.700	11.20	.952



TABLE XVI

Wedge

Hypersonic Similarity

4° Angle of Attack

<u>5° δ</u>				<u>10° δ</u>			
M	C _{Pu}	M	C _{PL}	M	C _{Pu}	M	C _{PL}
		2.64	.107	5.70	.0045	1.90	.197
		3.55	.083	11.40	.0035	2.54	.159
		4.40	.070			3.16	.134
		5.26	.062			3.80	.118
		7.03	.052			5.06	.099
		8.80	.046			6.34	.089
		13.10	.039			9.50	.075
						12.60	.069



TABLE XVI (continued)

Wedge

Hypersonic Similarity

4° Angle of Attack

<u>20°δ</u>				<u>30°δ</u>			
M	C _{Pu}	M	C _{PL}	M	C _{Pu}	M	C _{PL}
1.90	.125	2.01	.354	2.06	.243	2.52	.475
2.86	.088	2.41	.294	2.58	.210	2.91	.421
3.80	.070	3.21	.247	3.10	.185	4.36	.356
4.76	.059	4.01	.220	4.13	.155	5.80	.329
5.70	.052	6.01	.185	5.16	.138	8.70	.307
7.60	.044	8.02	.171	7.71	.118	11.60	.298
9.50	.039	12.00	.160	10.60	.103		
10.50	.033						

TABLE XVI (continued)

Wedge

Hypersonic Similarity

4° Angle of Attack

<u>40° δ</u>				<u>50° δ</u>			
M	C _{Pu}	M	C _{PL}	M	C _{Pu}	M	C _{PL}
2.09	.394	2.25	.705	2.08	.590	2.70	.925
2.79	.330	3.37	.595	2.60	.524	3.61	.854
3.49	.294	4.50	.550	3.90	.443	5.42	.796
5.21	.248	6.74	.514	5.20	.408	7.22	.773
6.96	.229	9.00	.498	7.80	.382	9.01	.760
10.50	.214	11.20	.490	10.40	.370	10.60	.753
				15.00	.564		

<u>60° δ</u>			
M	C _{Pu}	M	C _{PL}
2.05	.945	2.22	1.37
3.07	.715	2.96	1.26
4.10	.630	4.45	1.18
6.15	.616	5.92	1.14
8.20	.598	7.40	1.12
10.20	.589	8.90	1.11
12.20	.580	10.70	1.11



TABLE XVII

Cone

Hypersonic Similarity

0° Angle of Attack

10°		20°		30°		40°		50°		60°	
M	C_p	M	C_p	M	C_p	M	C_p	M	C_p	M	C_p
7.54	.0227	3.74	.0945	2.47	.212	1.81	.336	1.97	.530	2.12	.610
10.50	.0205	5.21	.0849	3.64	.191	4.50	.505	2.61	.350	2.77	.765
15.90	.0183	6.90	.0795	4.55	.176	5.55	.260	3.42	.506	5.66	.729
		9.00	.0740	5.93	.166	4.57	.264	4.50	.482	4.78	.707
		11.83	.0704	7.83	.153	5.77	.251	5.67	.469	6.99	.695
				10.45	.154	7.53	.244	8.53	.460		
						11.00	.239				



TABLE XVIII

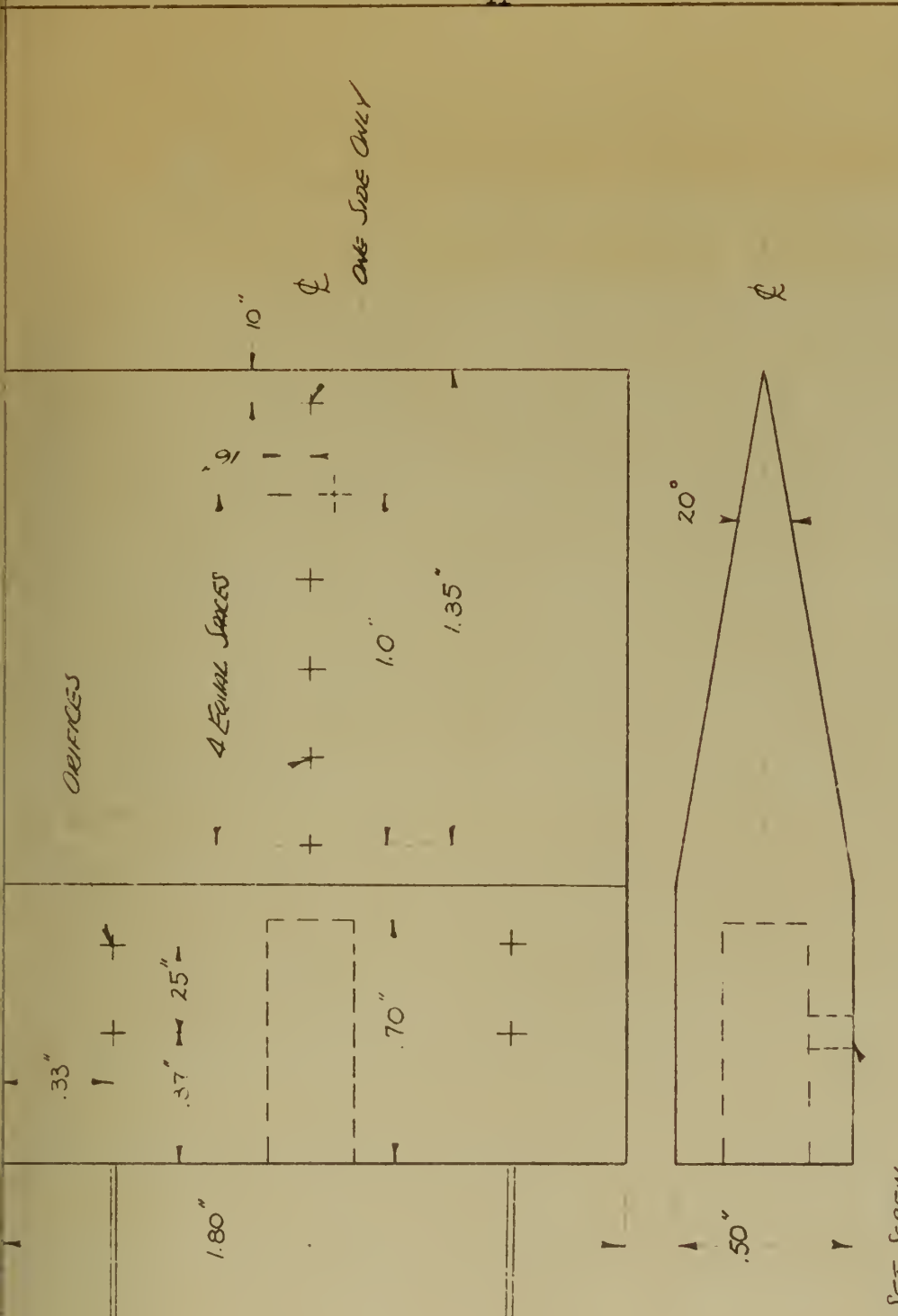
C_L vs M
 Wedge, $\delta = 20^\circ$

$\alpha = 2^\circ$

M	Oblique Shock	First Order	Second Order	Hypersonic Similitude
2.0	.1229	.0792	.1102	.0907
4.0	.0673	.0355	.0634	.0730
6.0	.0617	.0226	.0510	.0653
8.0	.0599	.0171	.0443	.0587
10.0	.0580	.0144	.0414	.0556
12.0	.0540	.0114	.0386	.0576

$\alpha = 4^\circ$

M	Oblique Shock	First Order	Second Order	Hypersonic Similitude
2.0	.2331	.1590	.2197	.2221
4.0	.1418	.0714	.1263	.1457
6.0	.1263	.0457	.1006	.1307
8.0	.1211	.0552	.0892	.1300
10.0	.1154	.0276	.0836	.1331
12.0	.1154	.0228	.0778	.1282



PART NO.	NAME	NO. ROD.	MATERIAL DESC.	MATERIAL SPEC.	WEIGHT
CALIFORNIA INSTITUTE OF TECHNOLOGY					
<i>FIG 1 WEDGE</i>					
<i>HYPERSONIC MODEL</i>					
DRAWN BY					
TRACED BY					
CHECKED BY					
APPROVED BY					
DATE					
COURSE NO.					
SECTION NO.					
SCALE <i>2"=1"</i>					
DWG. NO.					
NO.					

JET SCREW

FINISH

HEAT TREAT

ALL DIMENSIONS IN INCHES

LIMIT ON DIMENSIONS

UNLESS OTHERWISE NOTED

ANGULAR $\pm \frac{1}{2}^\circ$

FRACTIONAL $\pm \frac{1}{32}$

DECIMAL $\pm .010$

NUMBERS ARE SURFACE ROUGHNESS IN MICROINCHES

\sqrt{R} ROUGH MACHINE FINISH

$\sqrt{250}$ SMOOTH MACHINE FINISH

$\sqrt{40}$ ROUGH GRIND

$\sqrt{16}$ FINISH GRIND

$\sqrt{2}$ FINE GRIND, LAP

$\sqrt{1/4}$ POLISH





Fig. 3 - 20° WEDGE



Fig. 4 - 20° CONE

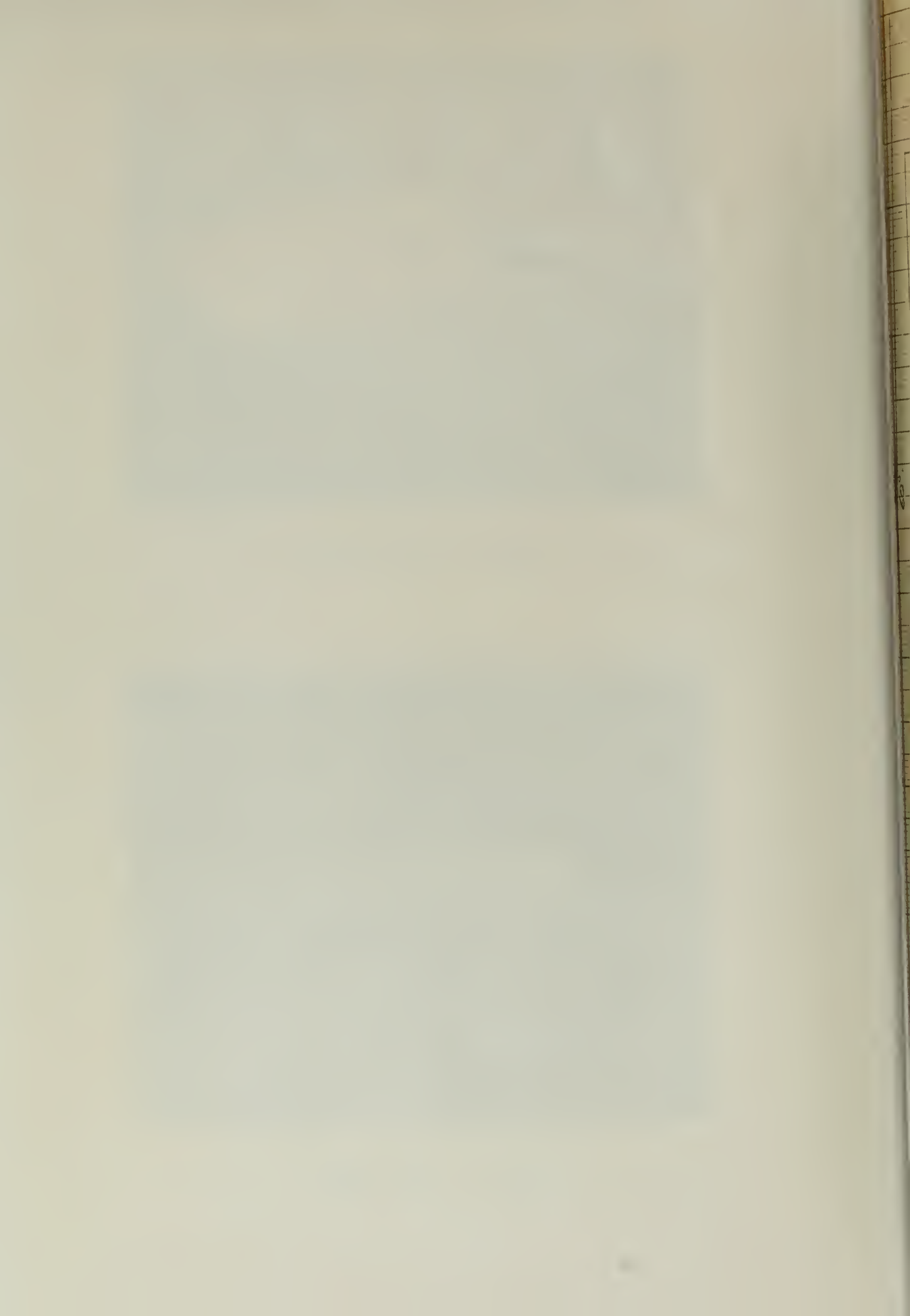
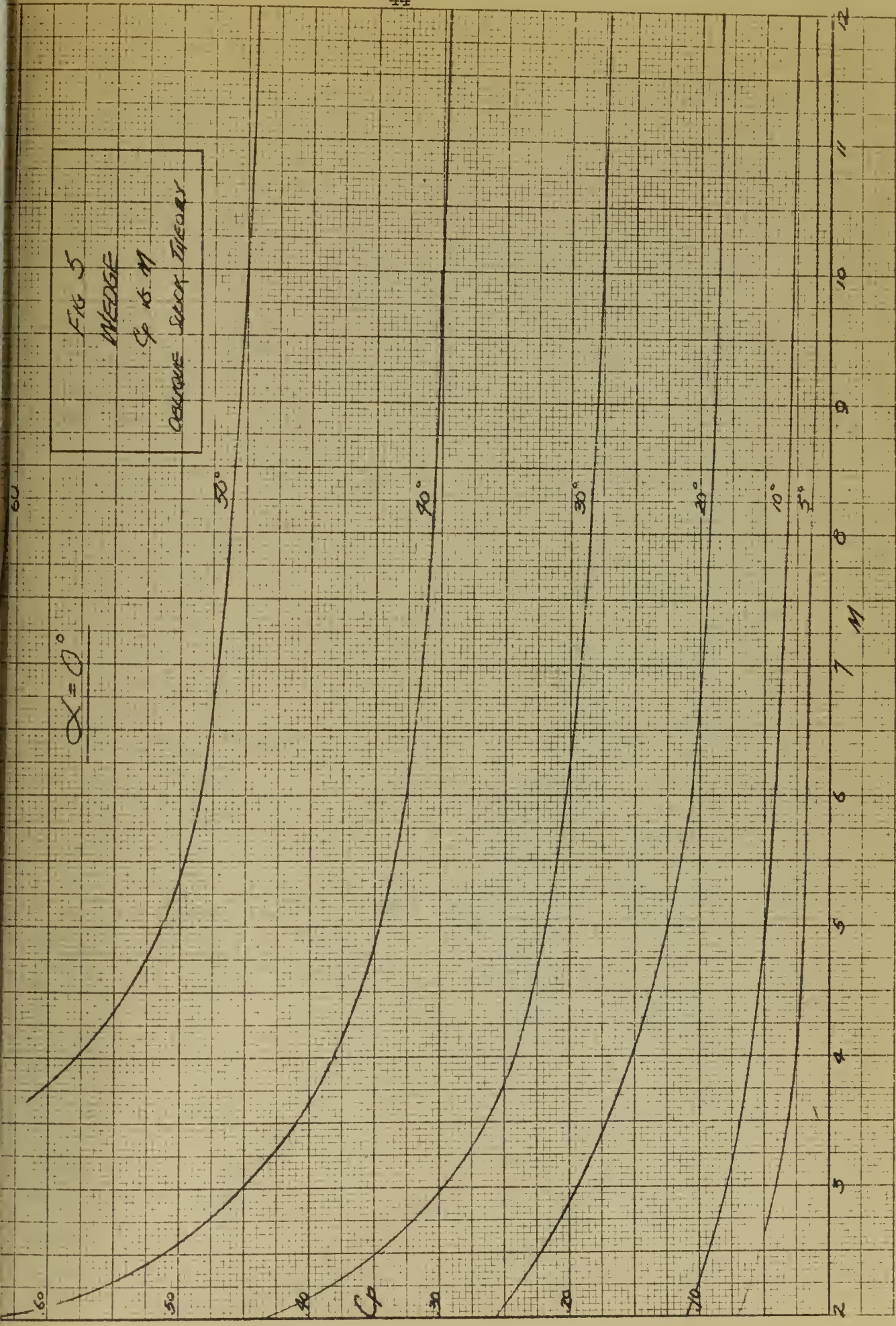


FIG 5
 WEDGE
 Sp 15 M
 DELTA SURFACE THEORY

$\alpha = 0^\circ$

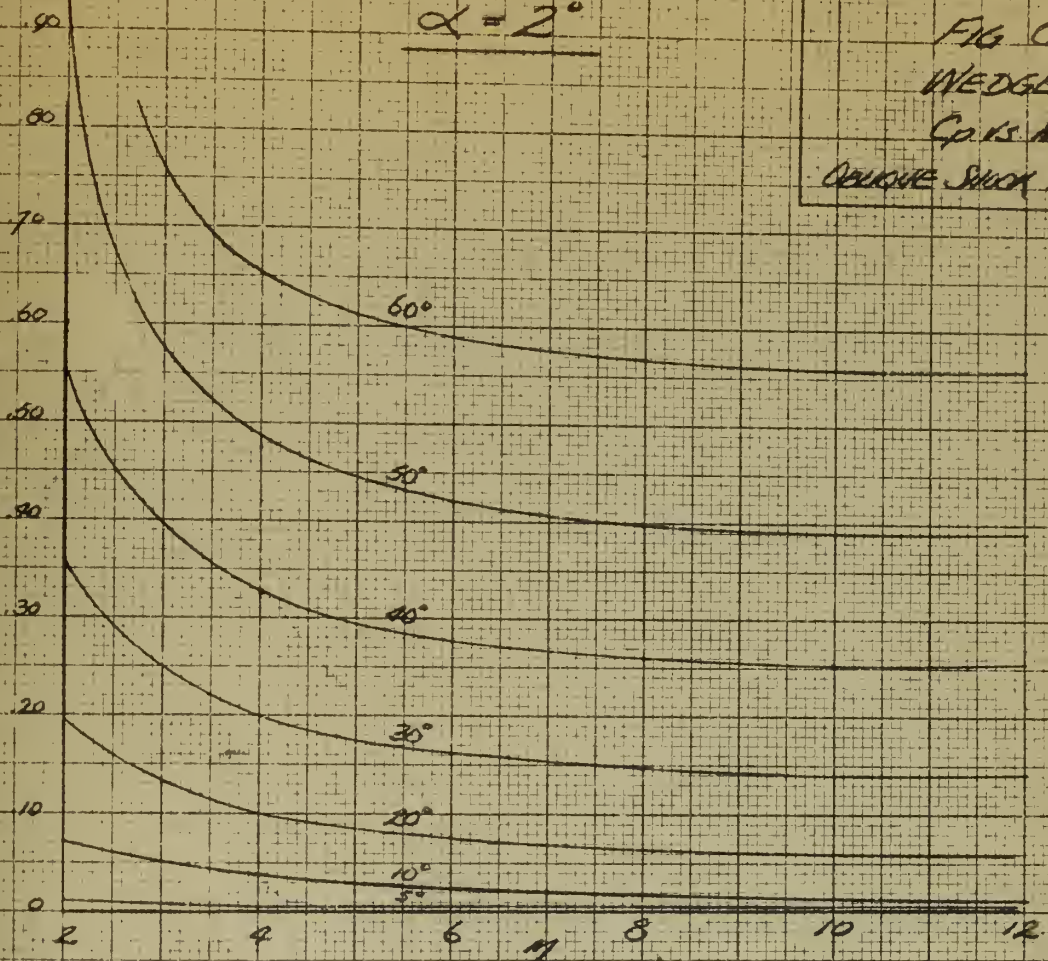




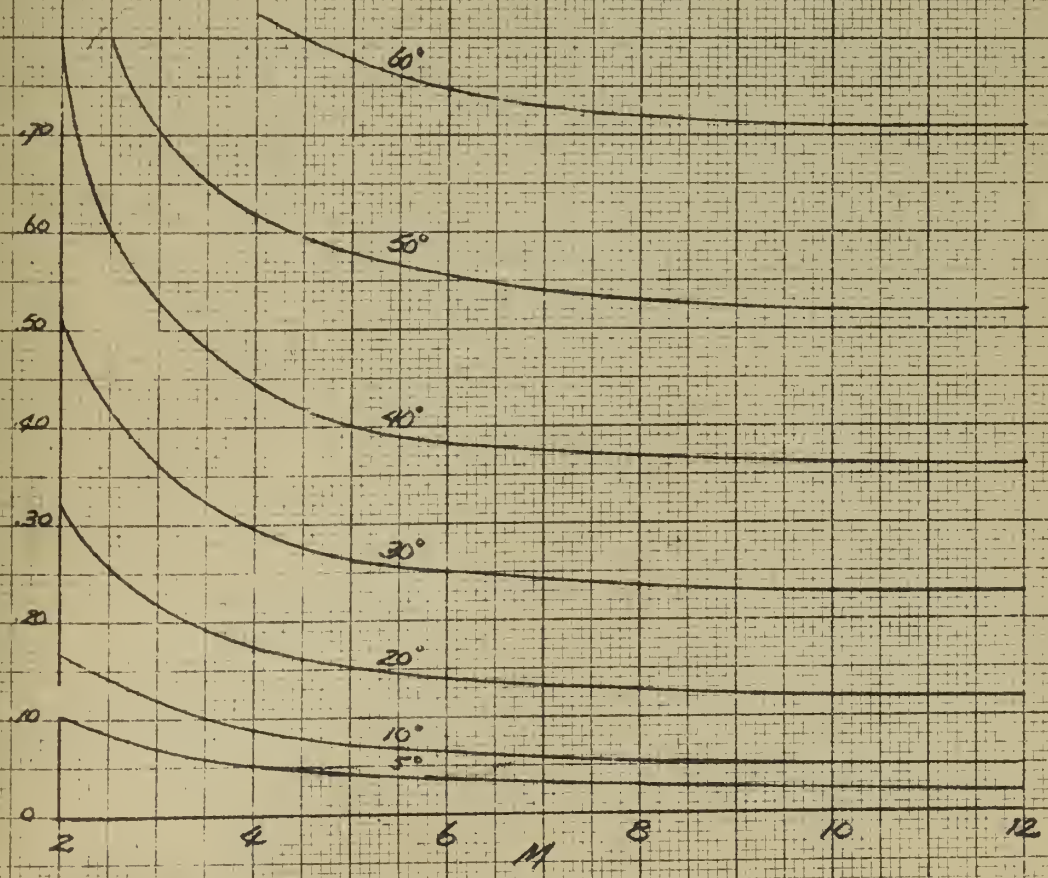
$\alpha = 2^\circ$

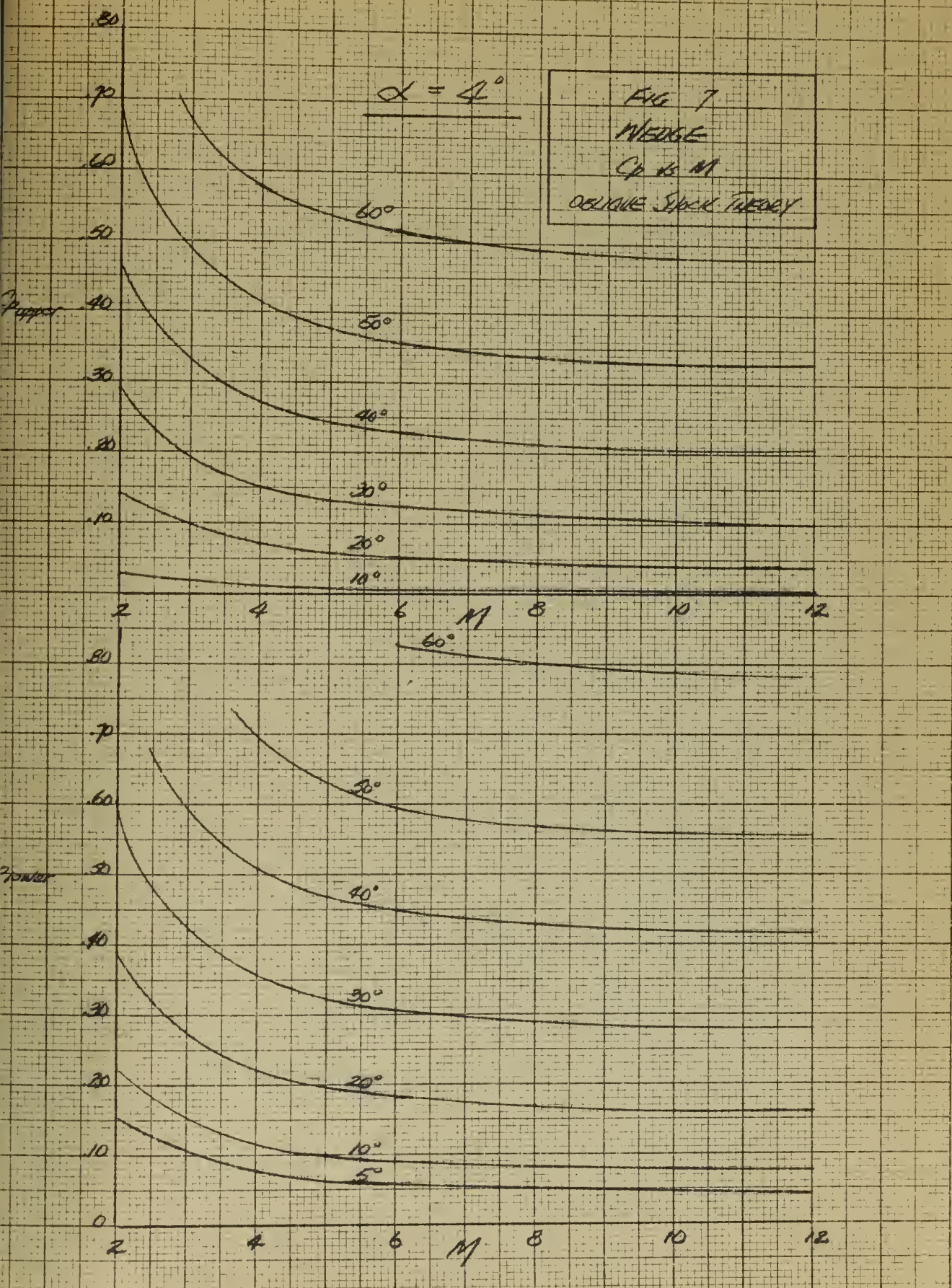
FIG 6
WEDGE
Cp 13 M
CALCULATED SHOCK THEORY

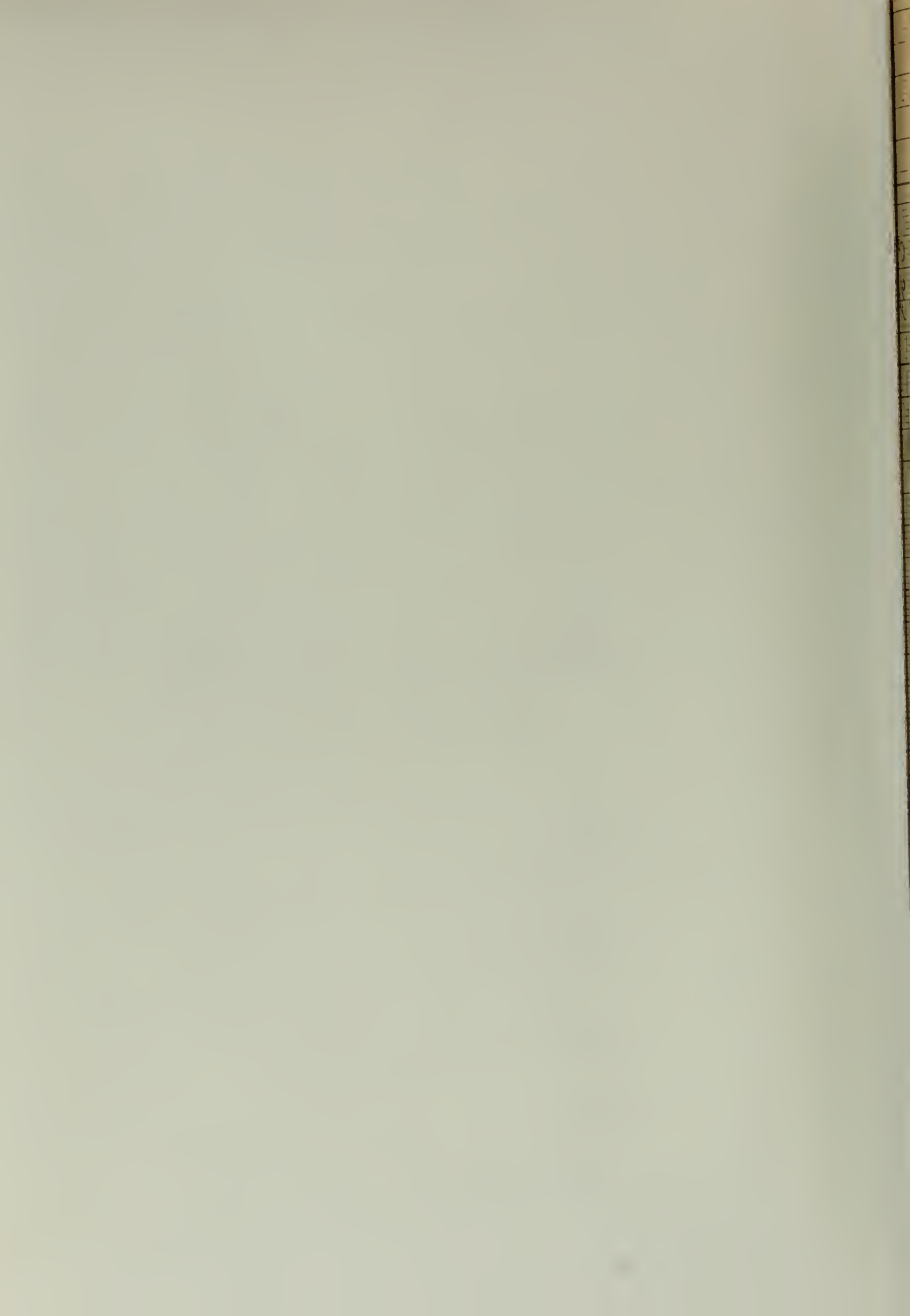
Copper



Aluminum







$\alpha = 0^\circ$
 CONE
 C_p vs M
 Exact Theory

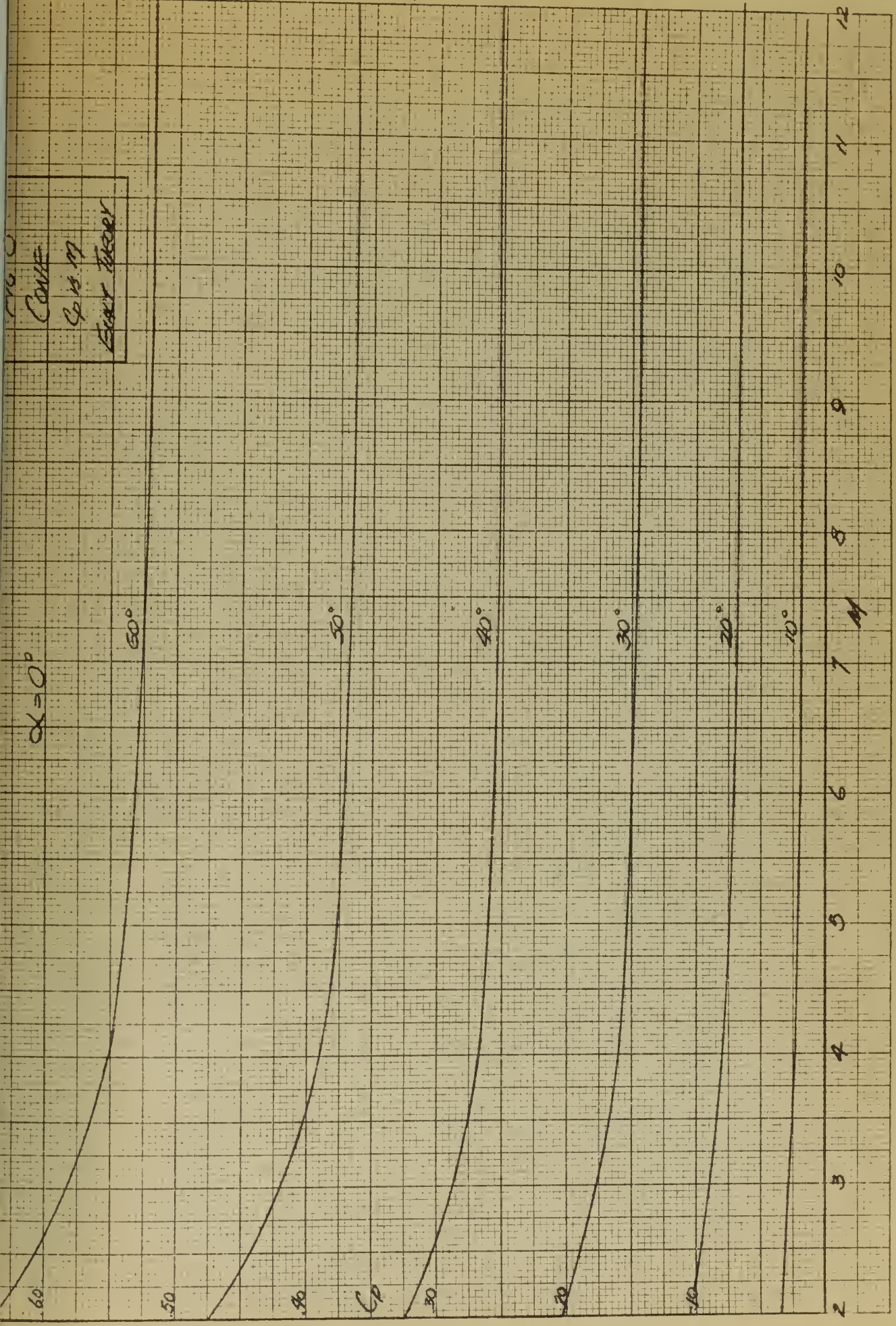
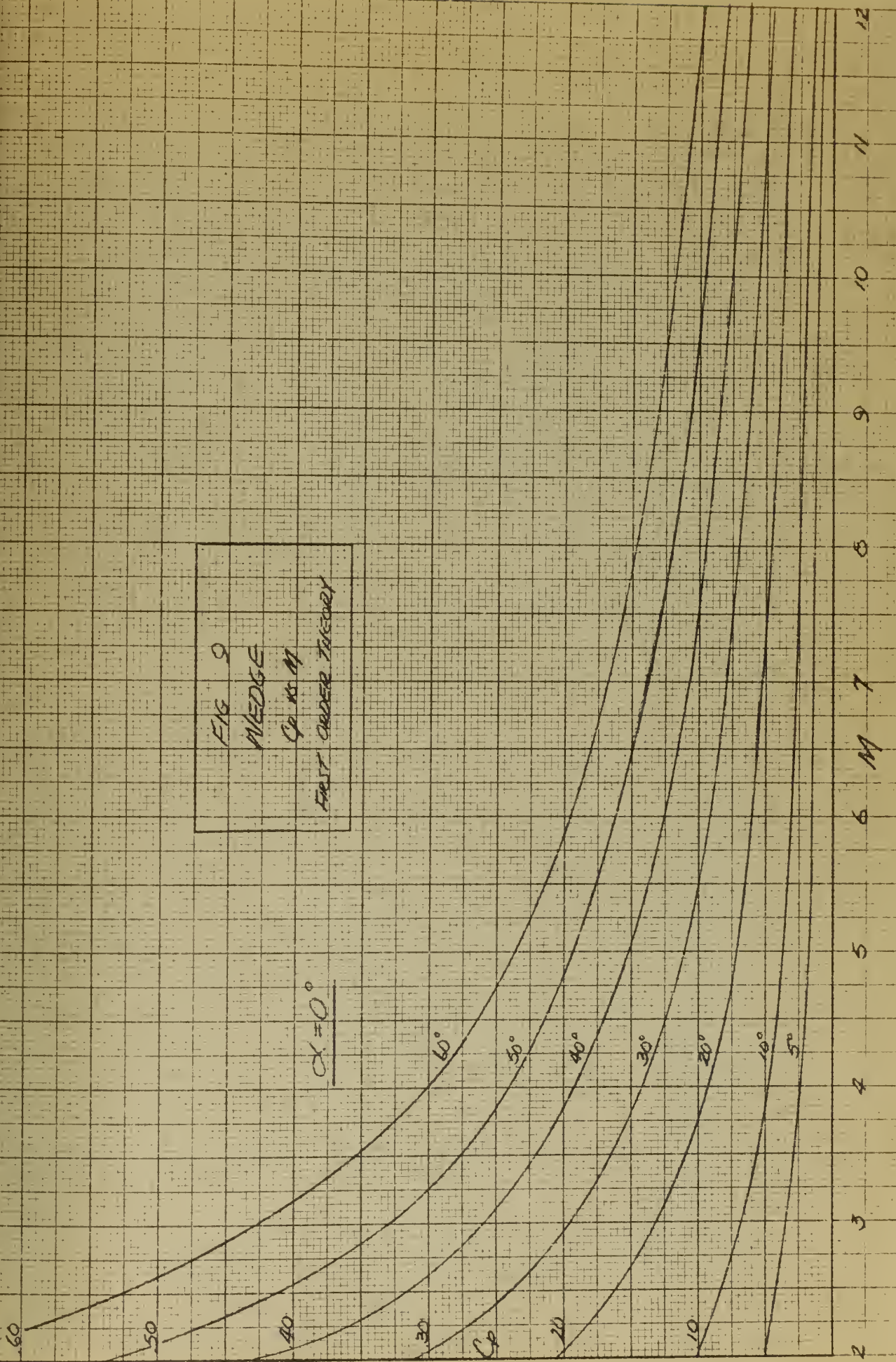
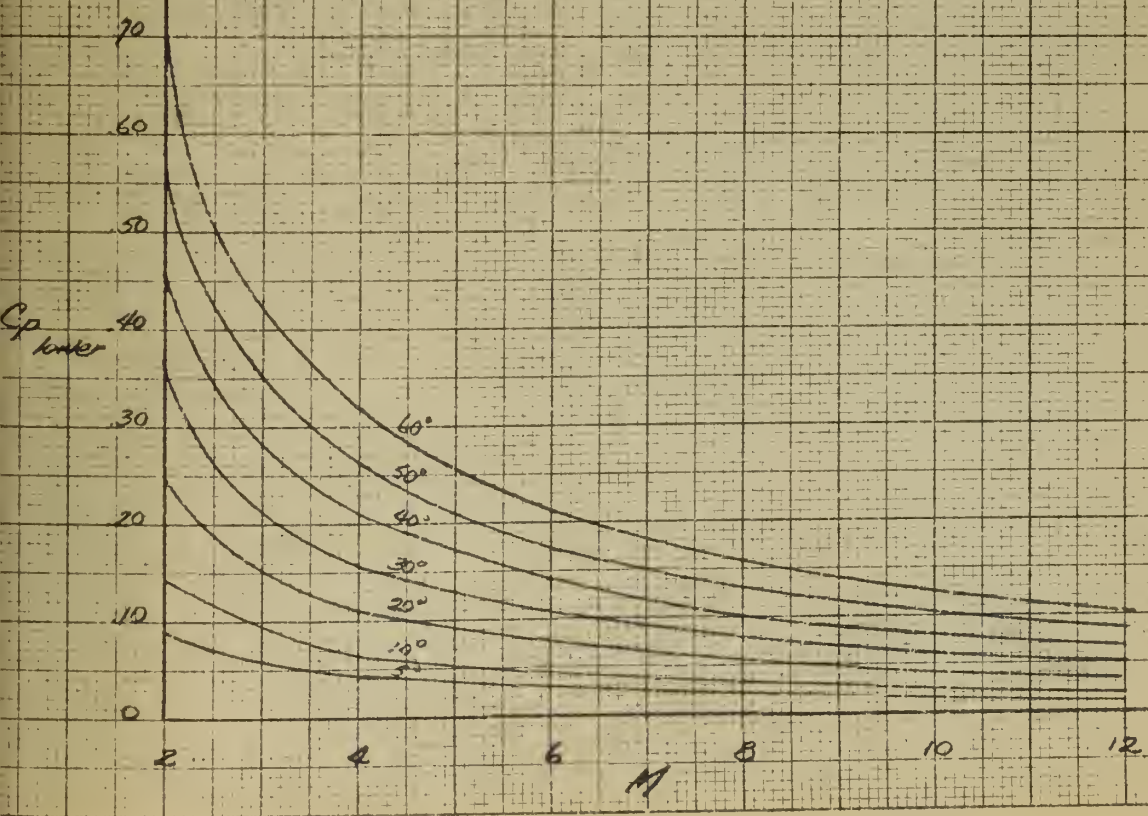
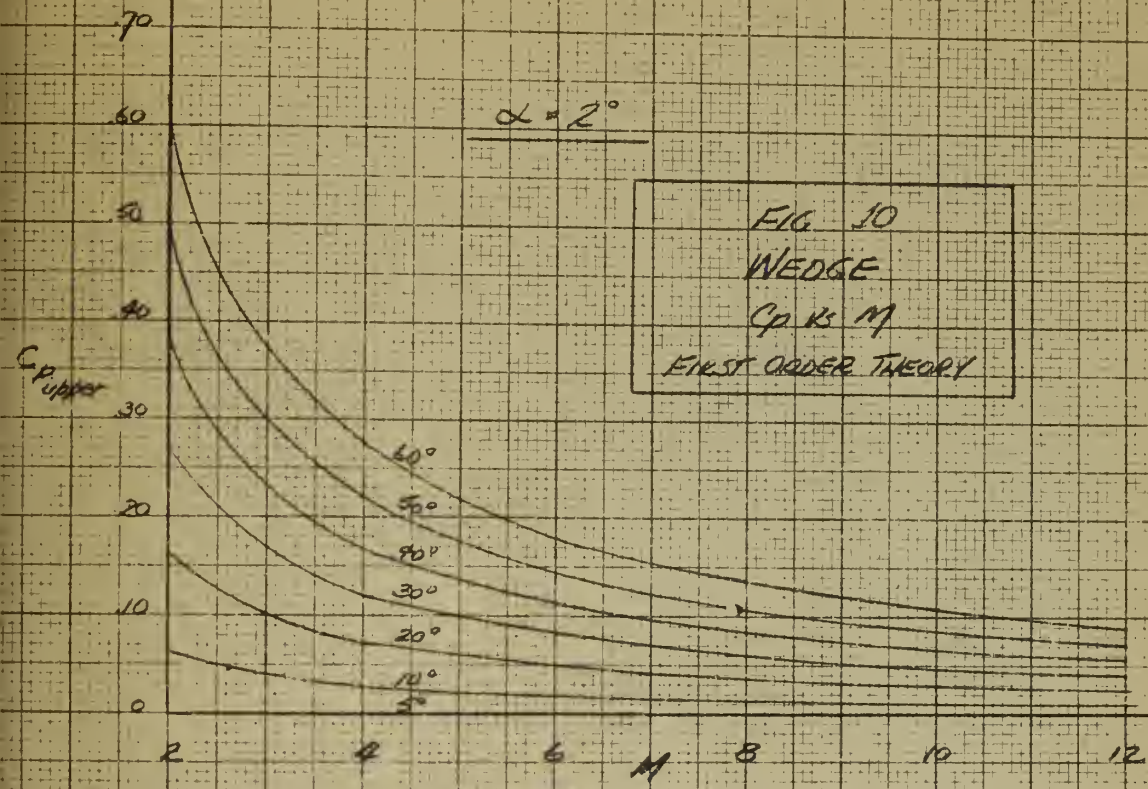


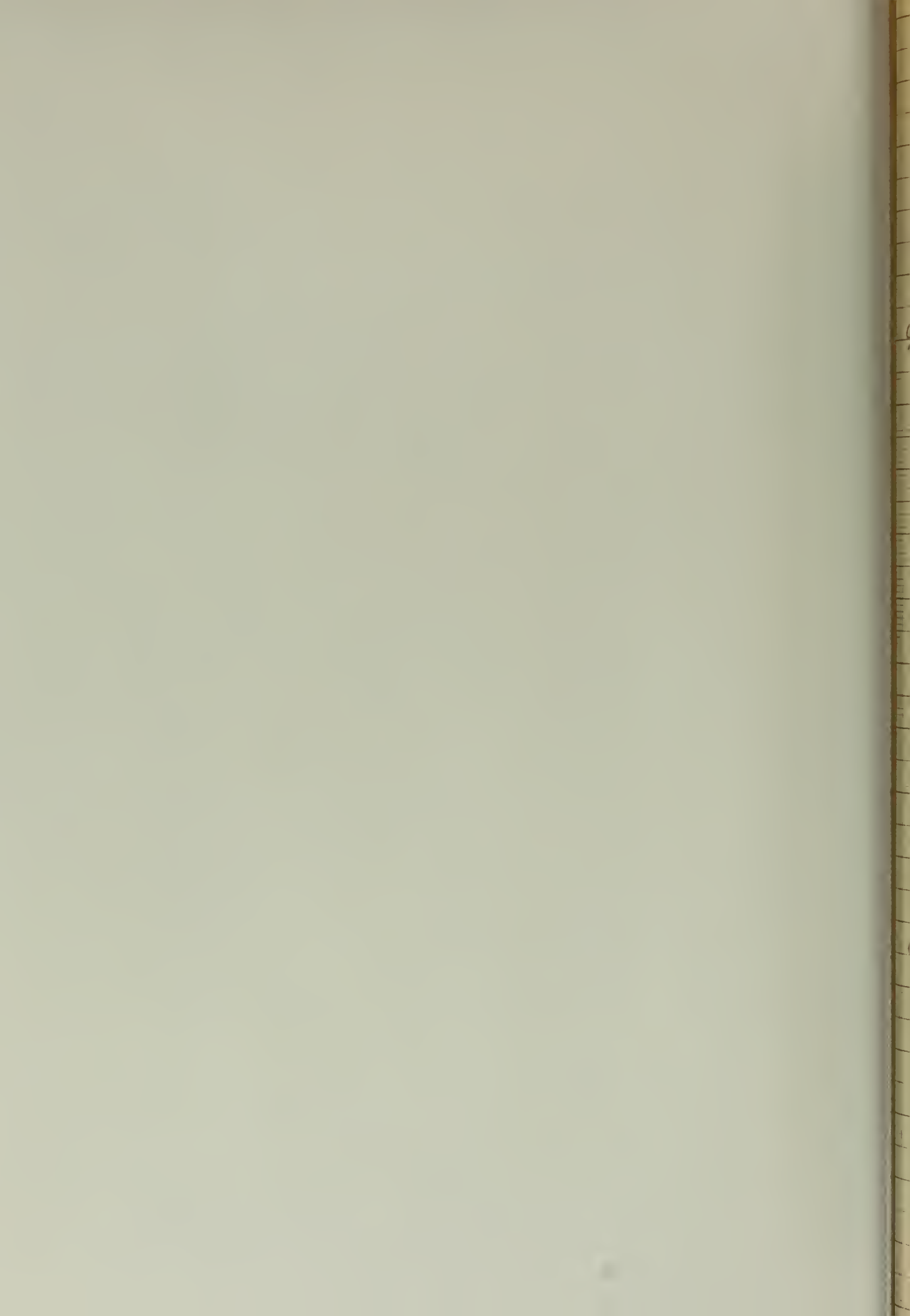


FIG 9
 WEDGE
 Cp vs M
 FIRST ORDER THEORY









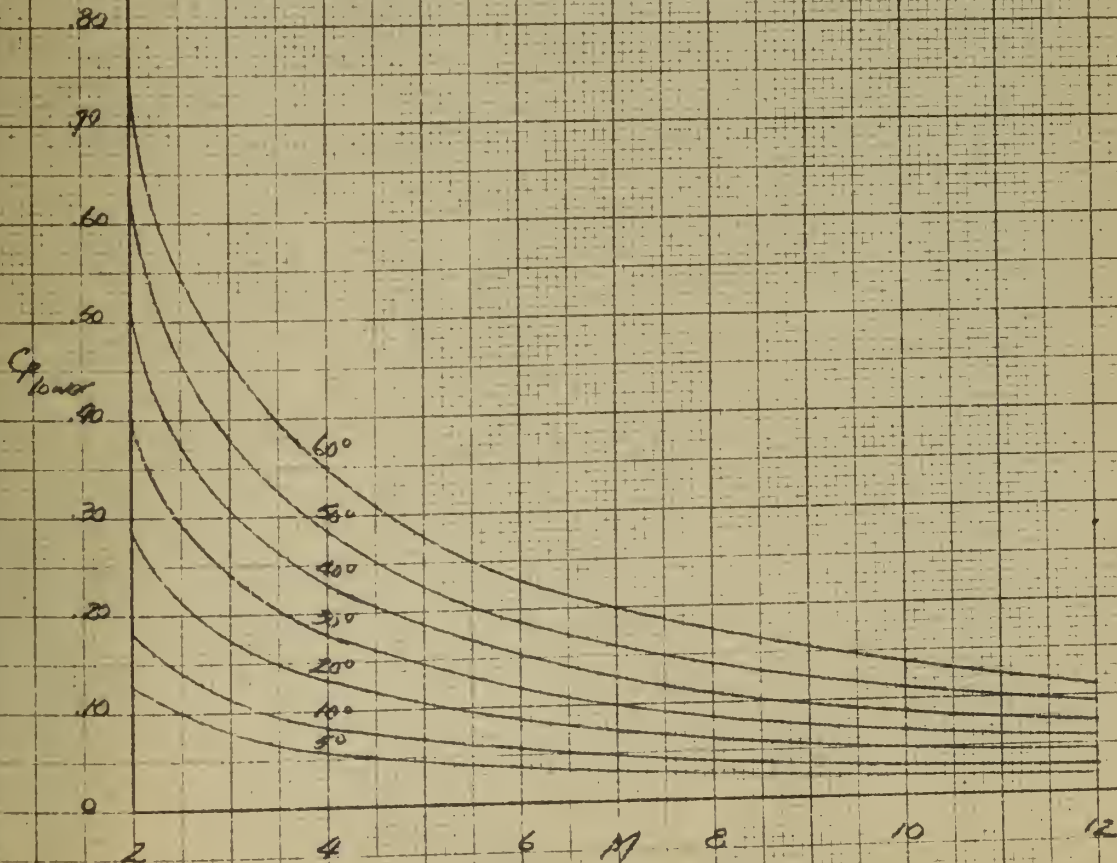
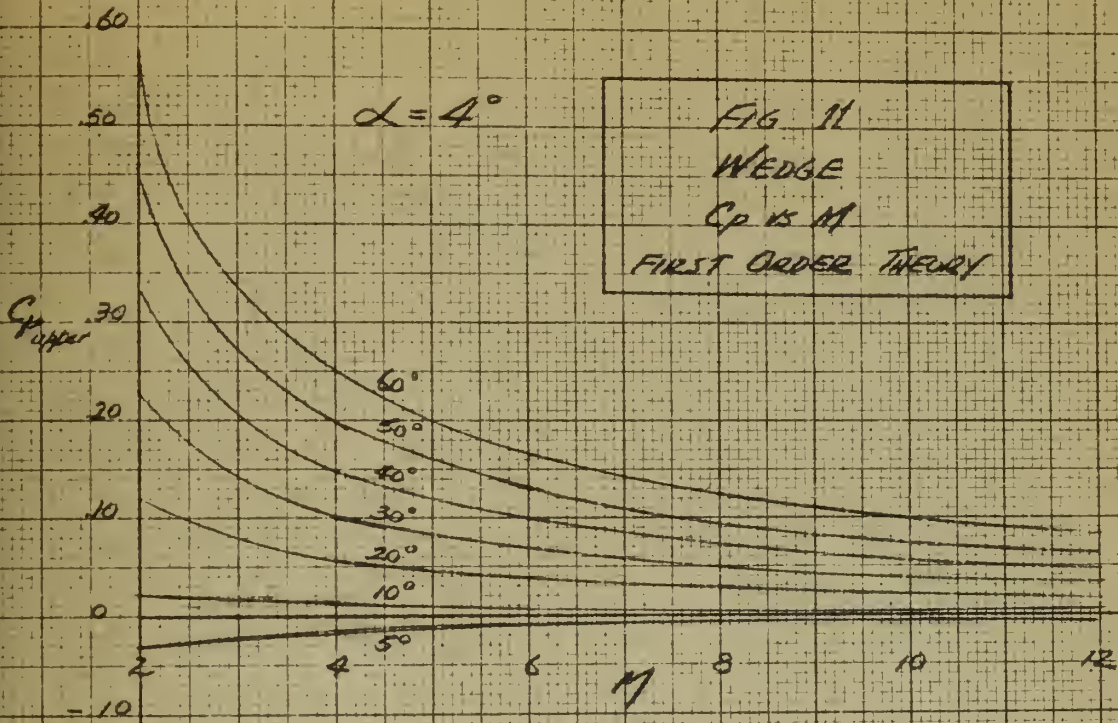




FIG 12
 CONE
 Cp vs M
 FIRST ORDER THEORY

$\alpha = 0^\circ$

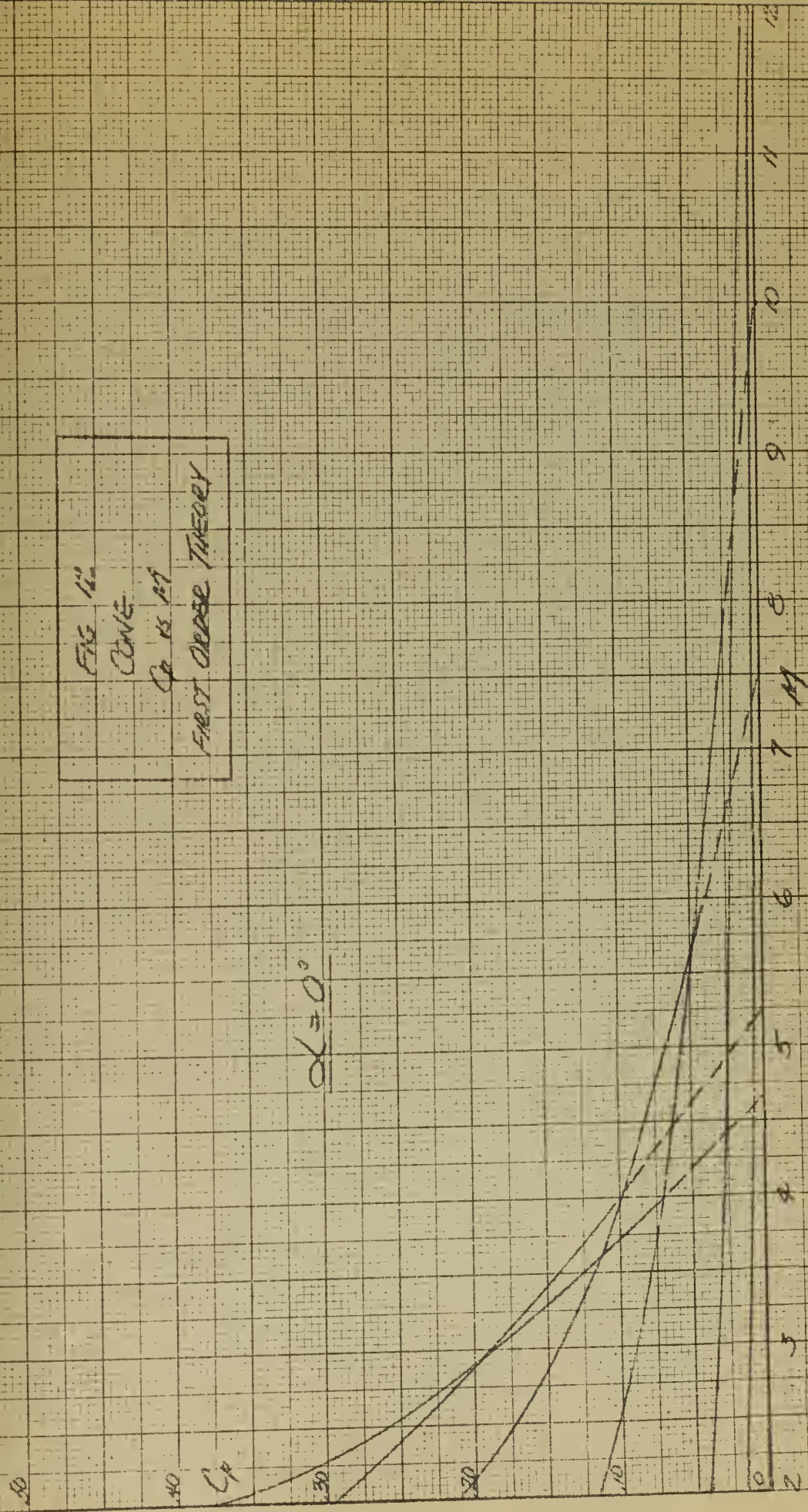
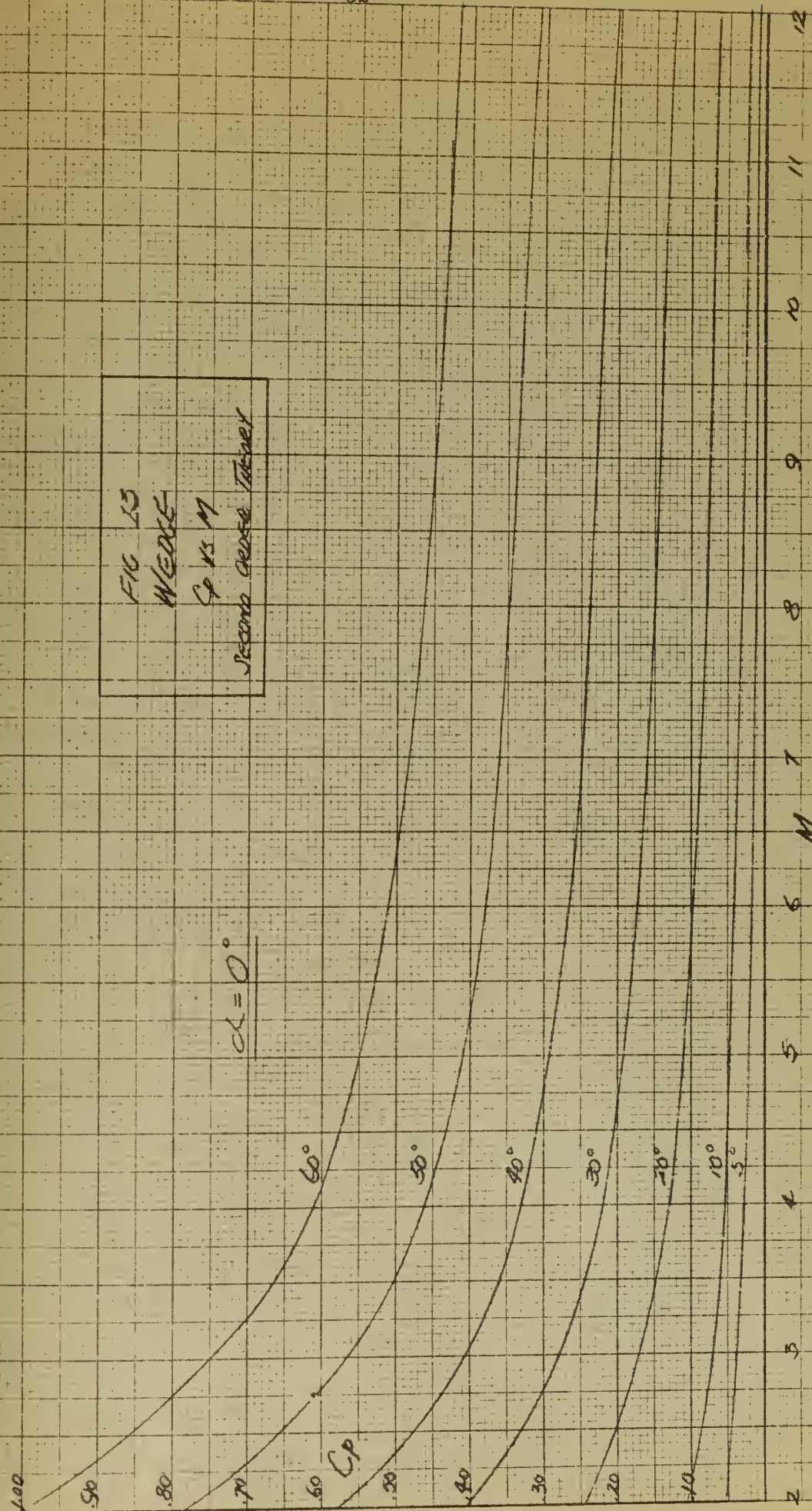




FIG 13
 WEGE-
 Sp vs M
 Second course Tabular

$CL = 0^\circ$



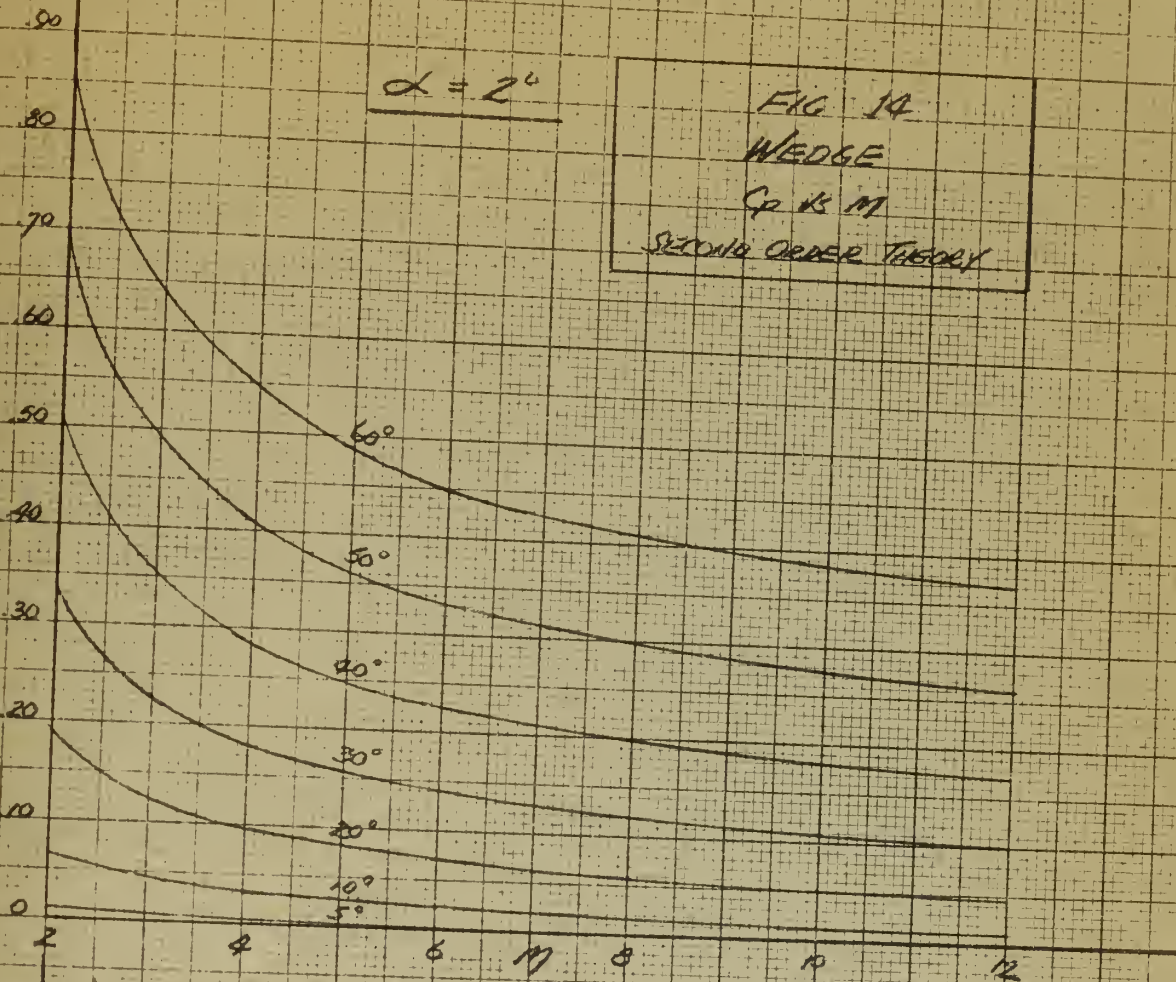
12
11
10
9
8
7
6 M
5
4
3
2



$\alpha = 2^\circ$

FIG 14
WEDGE
Cp vs M
SECOND ORDER THEORY

Cp upper



Cp lower

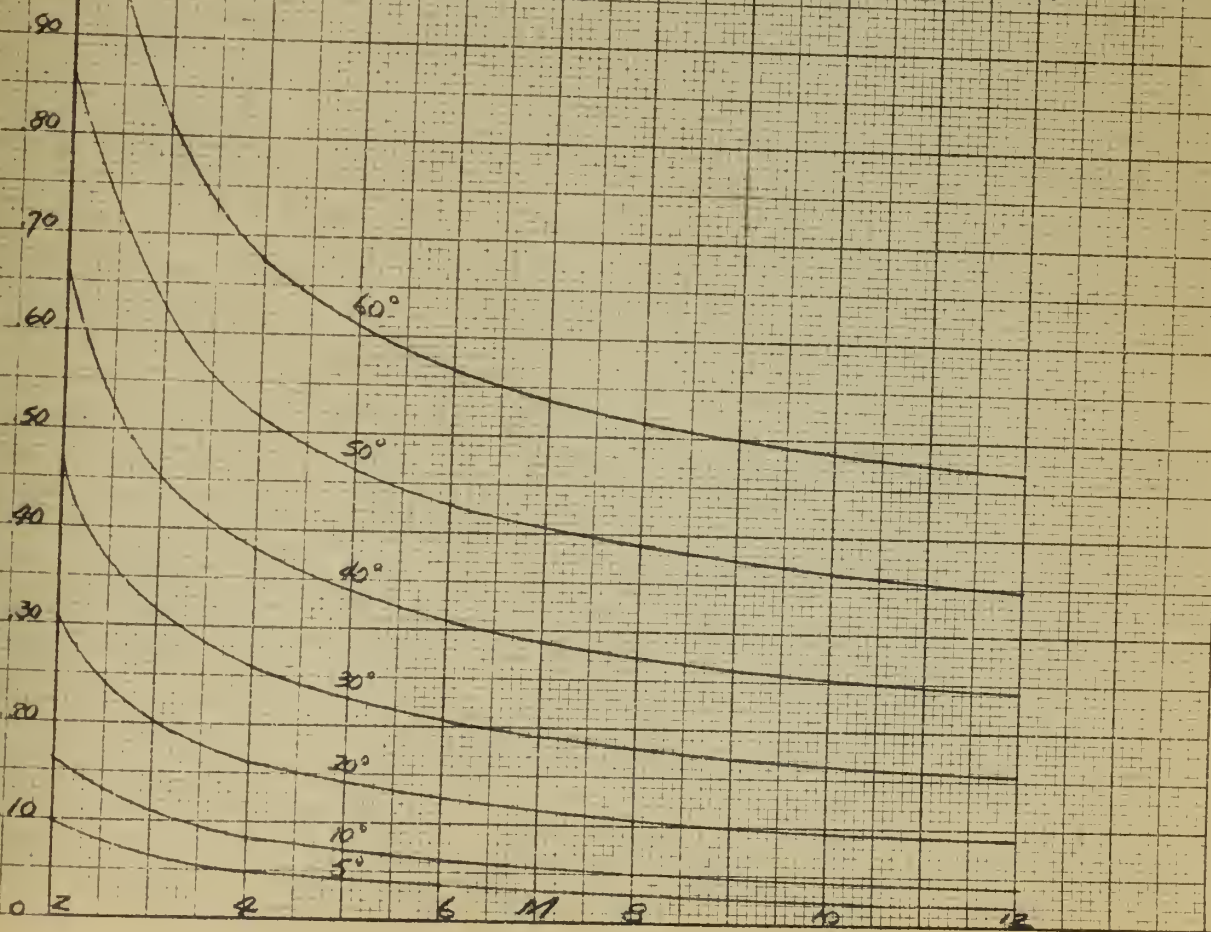


FIG 15
 WEDGE
 Cp 15 M
 SECOND ORDER THEORY

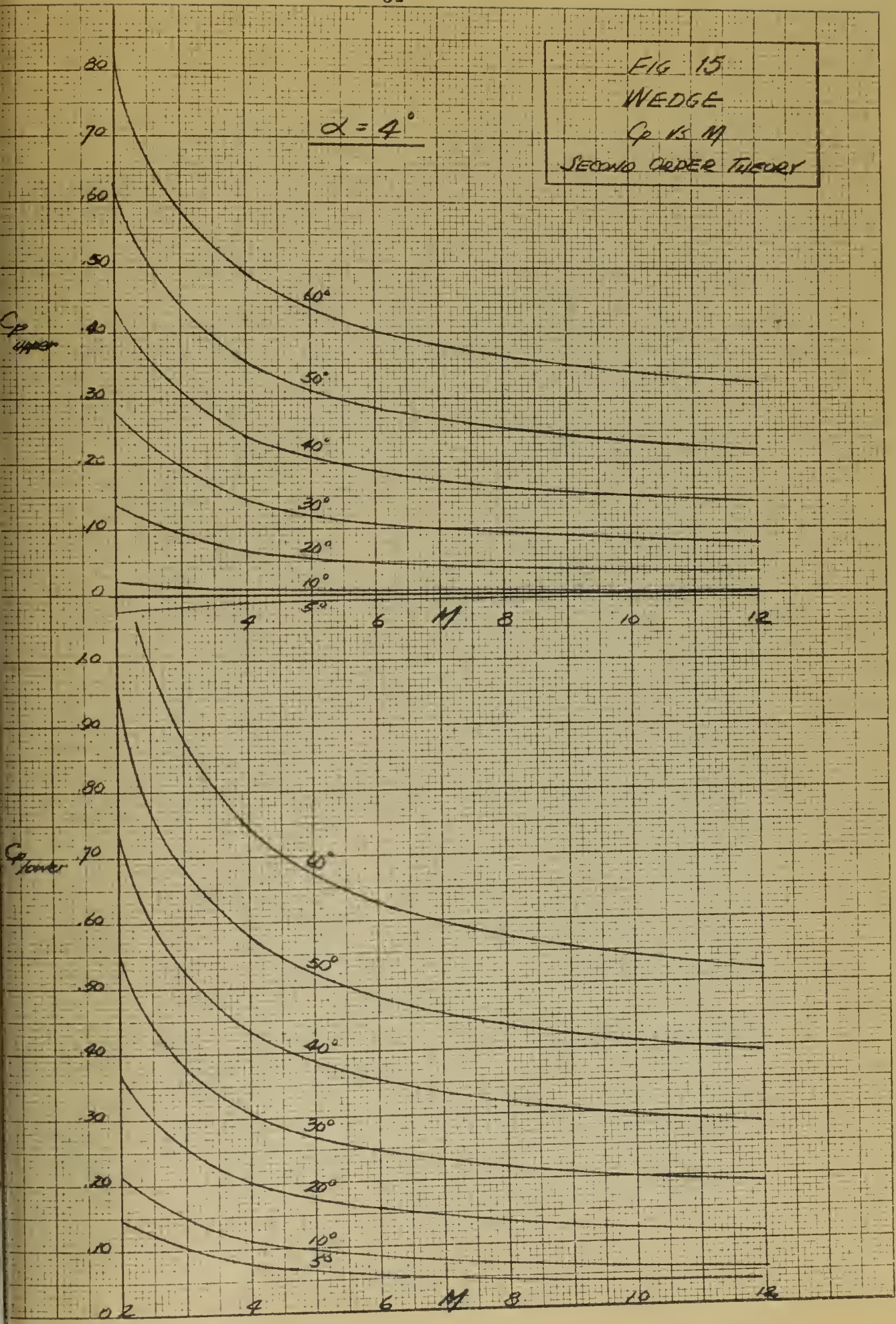
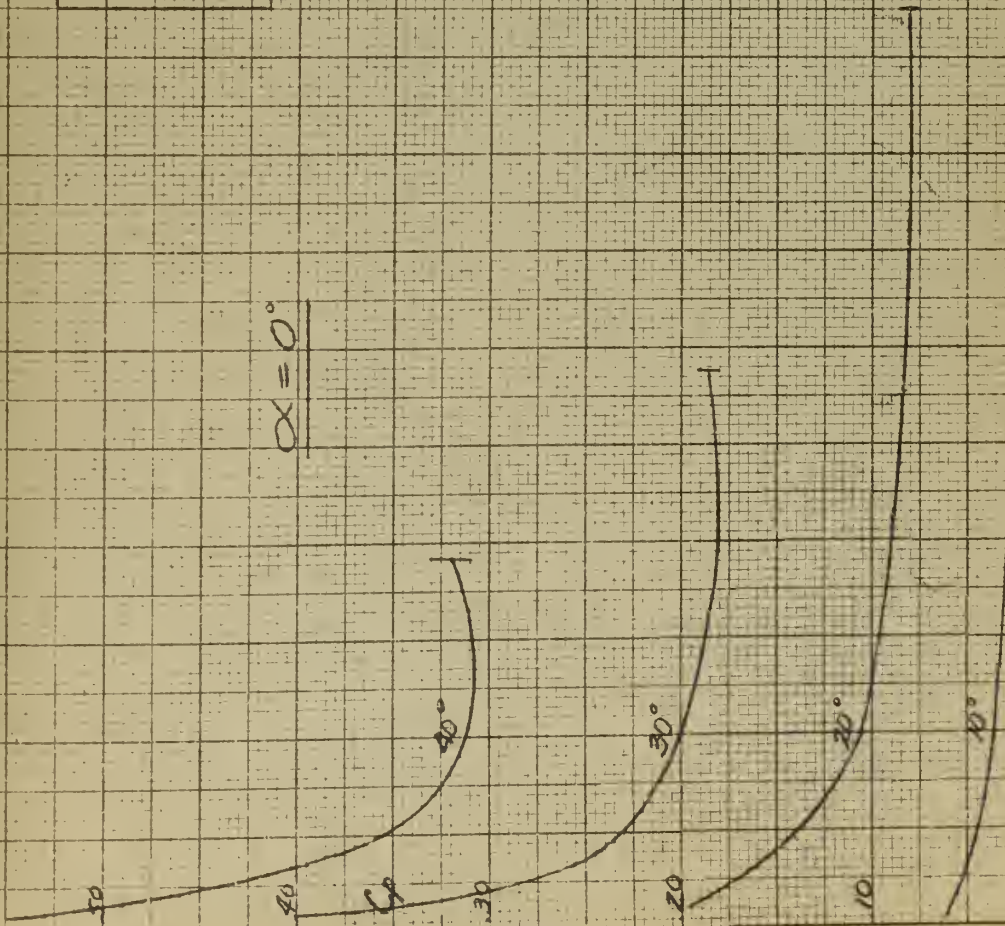




FIG 16
 CONE
 Cp vs M
 SECOND ORDER THEORY

$\alpha = 0^\circ$



11
10
9
8
7
6
M
5
4
3
2

FIG. 17
 AEROSOL SIMILARITY PARAMETERS

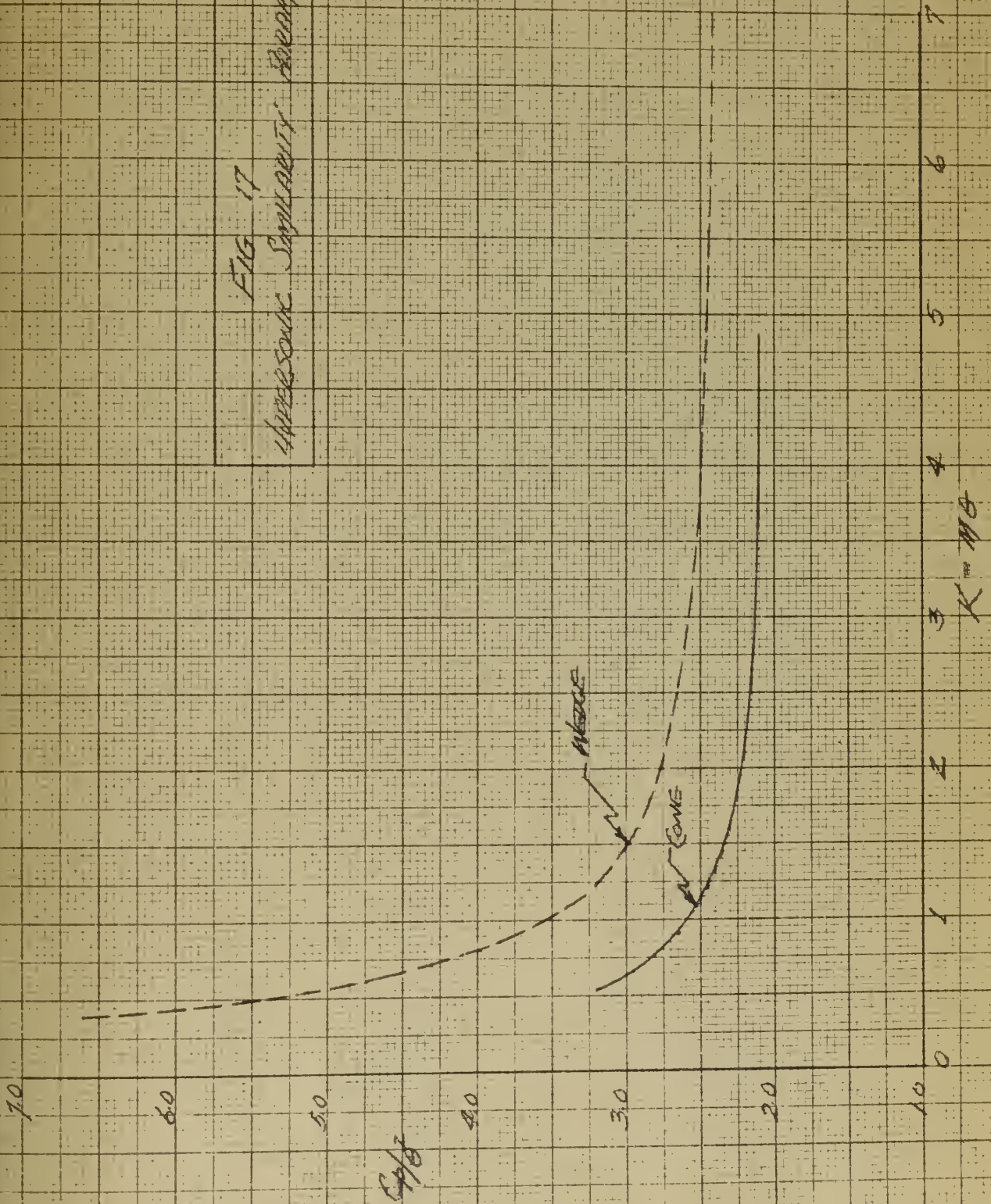


FIG A3

WEDGE

Cp to M

HYPERSONIC SIMILARITY

$\alpha = 0^\circ$

1.00

.90

.80

.70

Cp

.60

.50

.40

.30

.20

.10

0

60°

50°

40°

30°

20°

10°

5

4

3

2

1

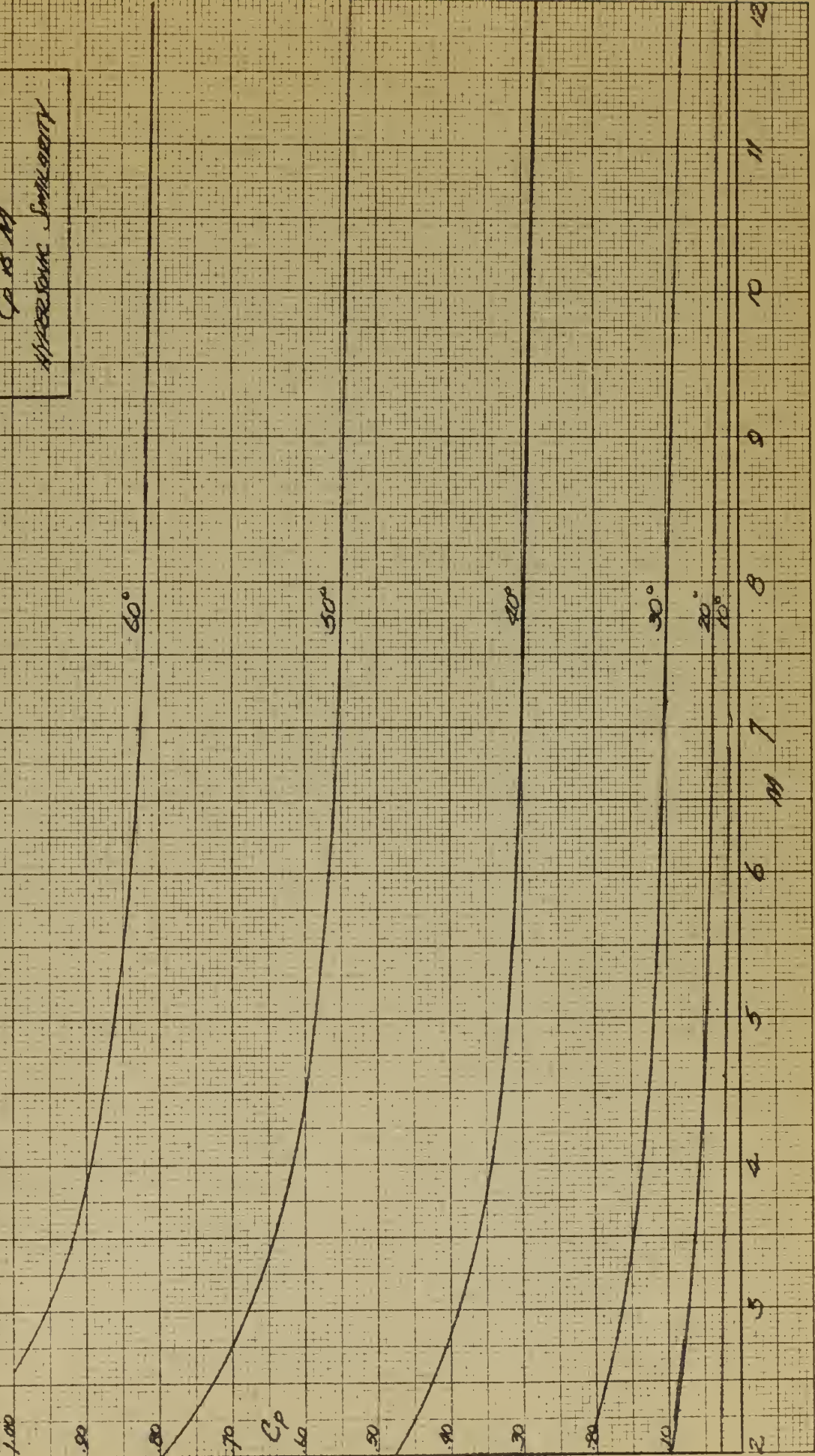
0

1

2

3

4



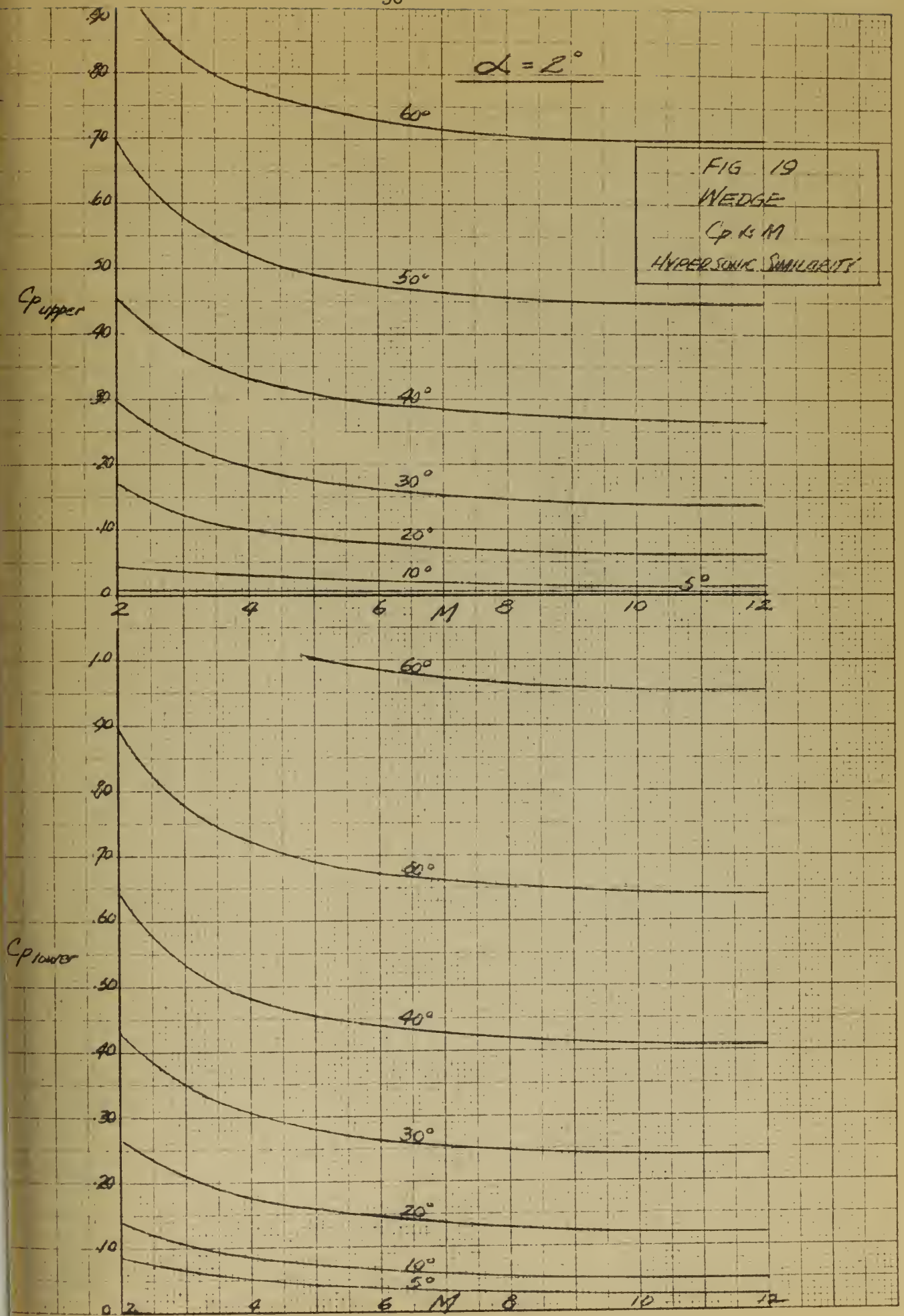


FIG 20
WEDGE
 C_p vs M
INFRASONIC SIMILARITY

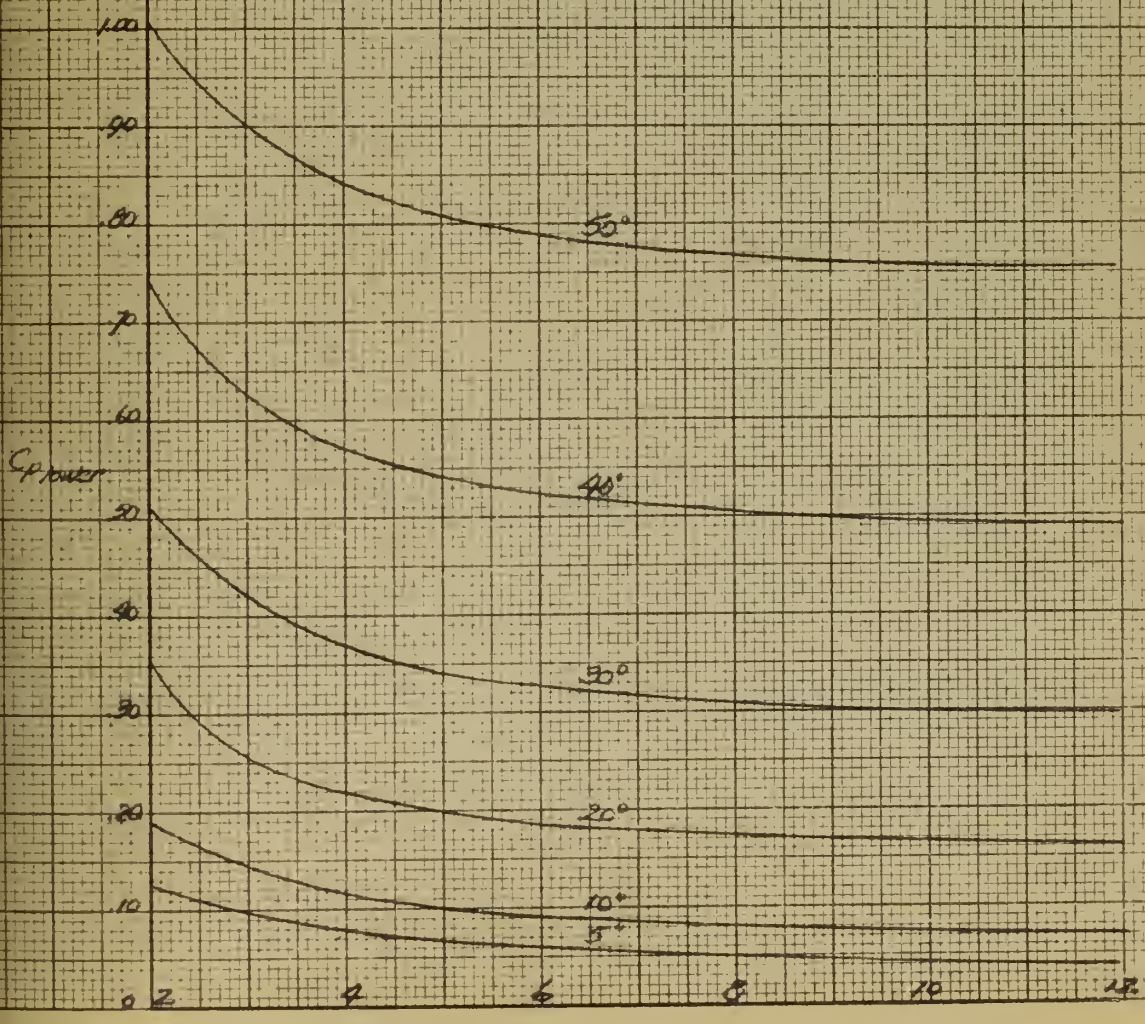
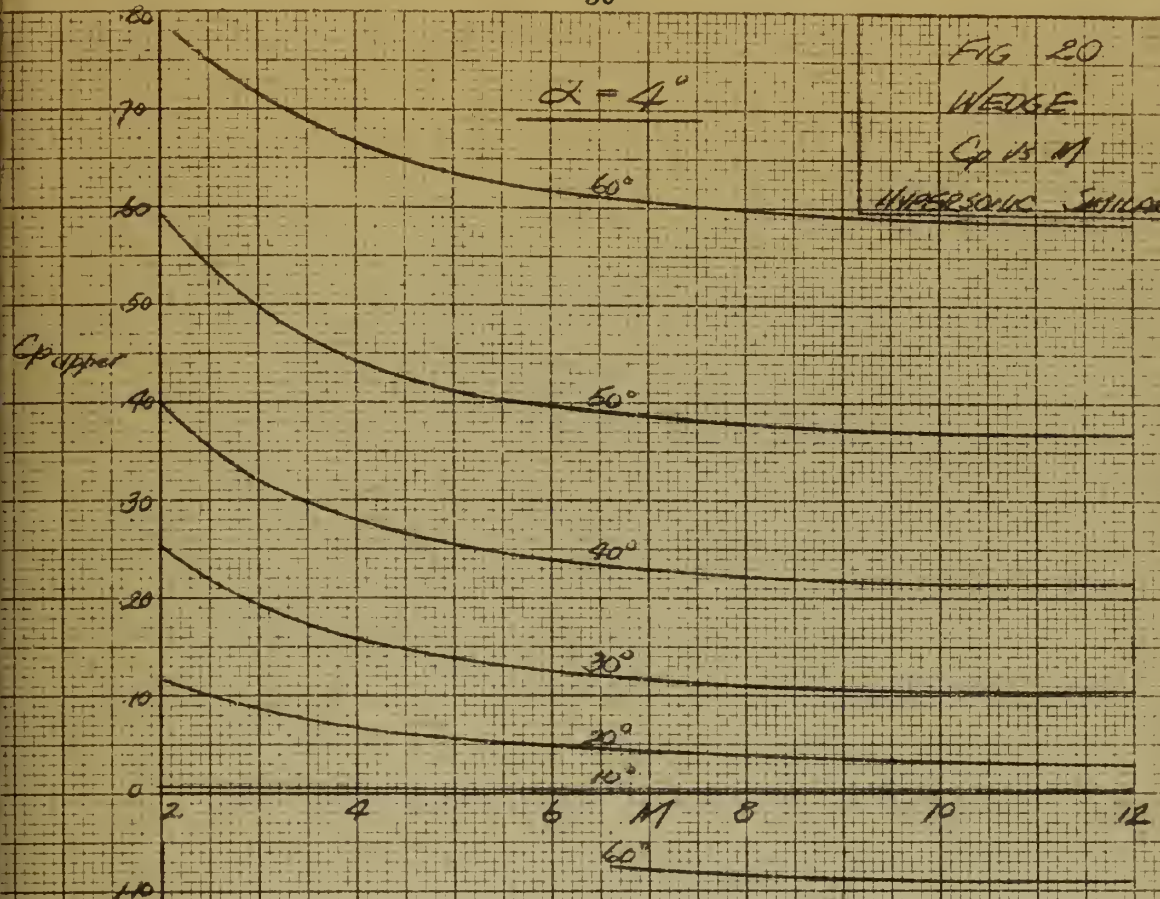




FIG 21
 CONE
 Sp at M
 HYPERBOLIC SIMILARITY

$\alpha = 0^\circ$

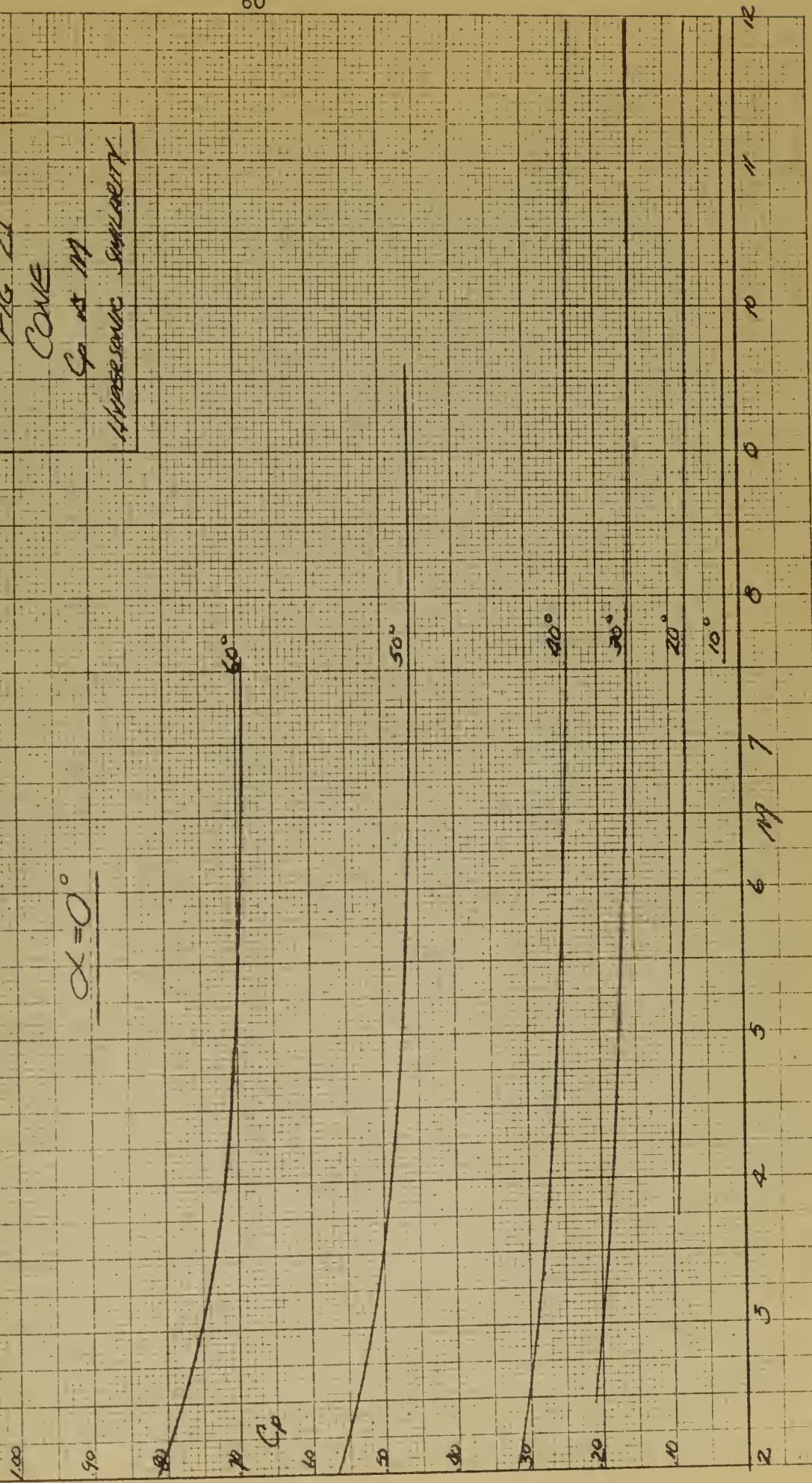
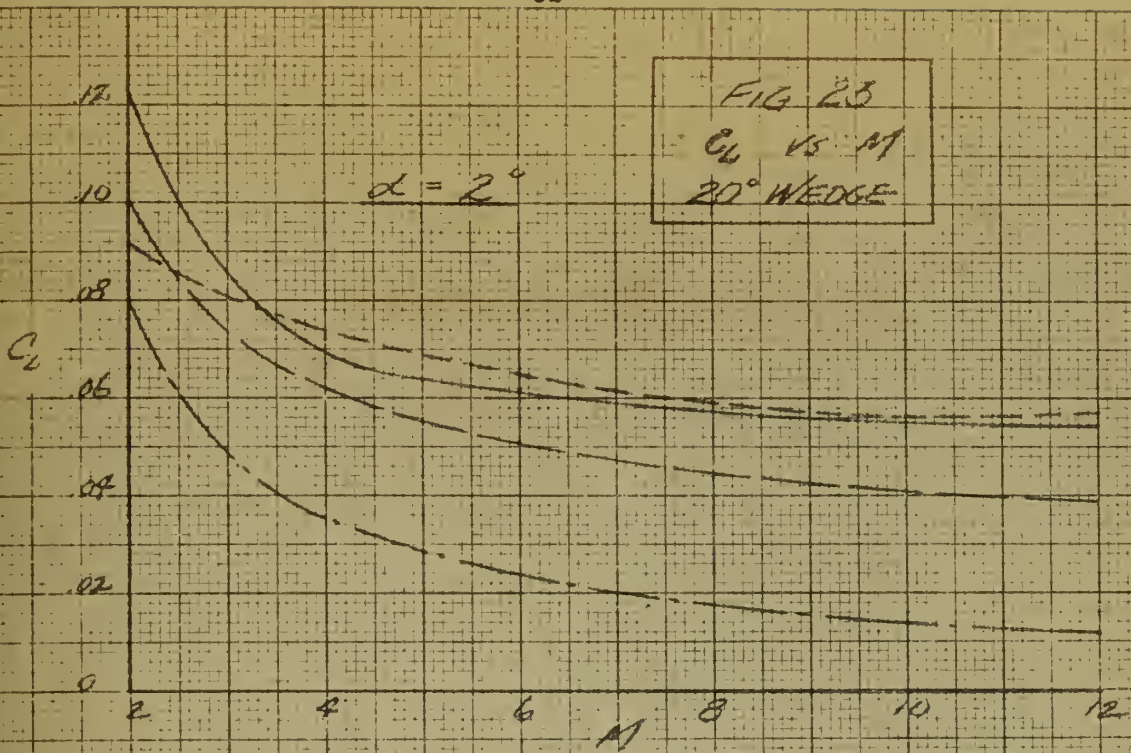


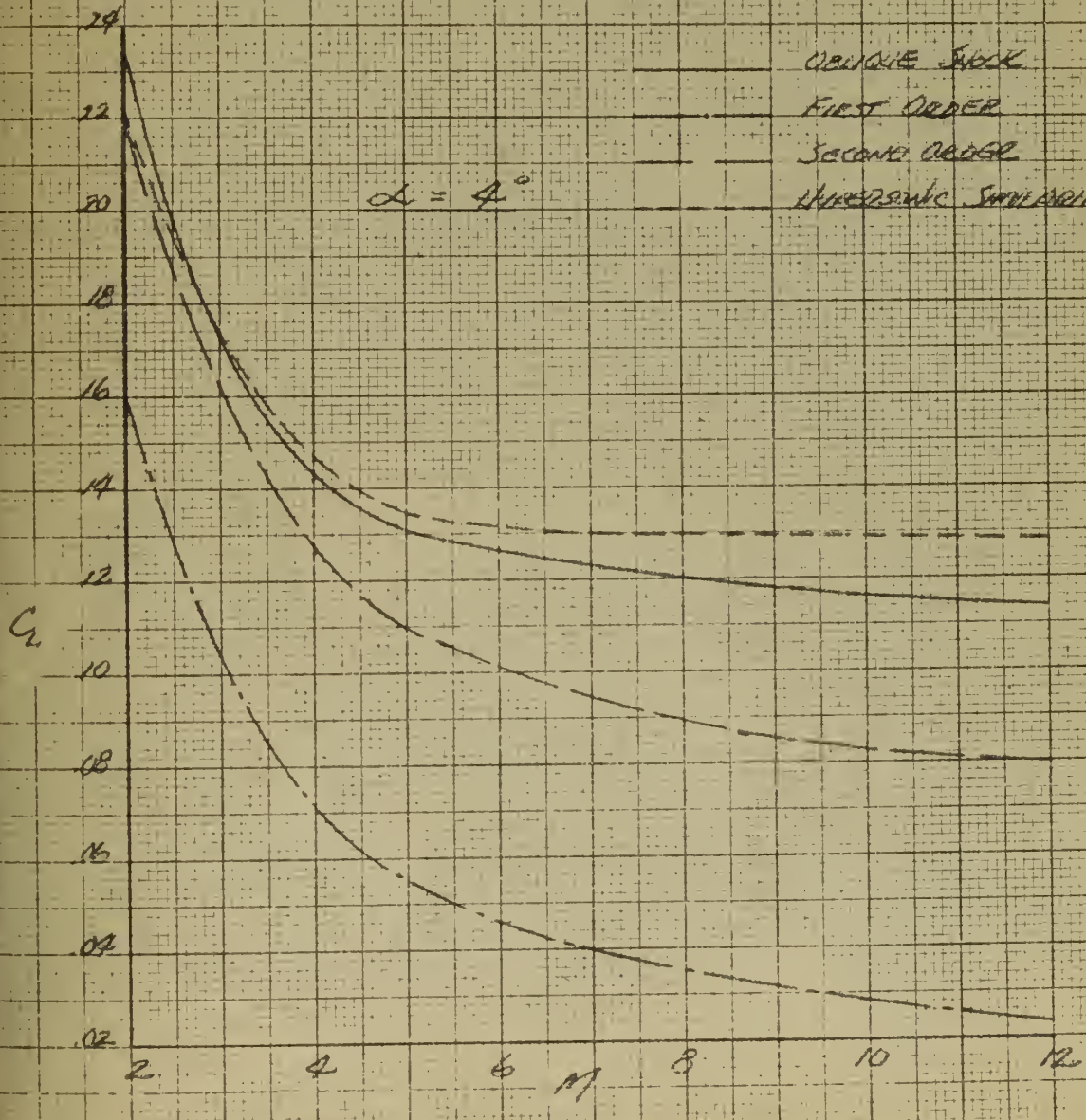
FIG 23
 C_L VS M
 20° WEDGE

$\alpha = 2^\circ$



$\alpha = 4^\circ$

OBLIQUE SHOCK
 FIRST ORDER
 SECOND ORDER
 HYPERSONIC SIMILARITY





Thesis
S33

Scherer

12992

Aerodynamic character-
istics of a wedge and
cone at hypersonic mach
numbers.

Thesis
S33

Scherer

12992

Aerodynamic character-
istics of a wedge and
cone at hypersonic mach
numbers.

thesS33

Aerodynamic characteristics of a wedge a



3 2768 002 00345 1

DUDLEY KNOX LIBRARY